Author:
Christer, Salomon

Title:
Investigating pathways of cell competition in Drosophila melanogaster

Investigating pathways of cell competition in *Drosophila melanogaster*

By

Salómon Christer

School of Cellular and Molecular Medicine

University of Bristol

A dissertation submitted to the University of Bristol

in accordance with the requirements for award of the degree of

Master of science by research

in the Faculty of Life Sciences

November 2020

Word Count: 15610

Abstract

Cell competition is an evolutionarily conserved process where cells compete and eliminate each other based on their relative fitness. In this interaction the fitter cells, termed "winners", eliminate less-fit "loser" cells, and increase proliferation to occupy the newly acquired niche. Cell competition is involved in various biological processes, including cancer, but despite its early discovery many aspects of what drives cells to compete remain elusive. Loser cells regularly exhibit chronic activation of stress signalling pathways such as the Unfolded protein response (UPR) and the oxidative stress response, making them useful markers for competition. They also play an active role in driving the loser status, where for example, overexpression of Nrf2, a component of the oxidative stress response is sufficient to confer the loser status in Drosophila. To understand how Nrf2 mediates the loser status, our lab investigated downstream targets of Nrf2 in a preliminary screen.

From the screen, the bZIP transcription factor: Abrupt emerged as a strong candidate as the expression of an *abrupt*-RNAi line (KK) in Drosophila wing-discs caused hyperactivation of both the UPR and Nrf2 and rapid elimination by surrounding WT cells in mosaic tissue. It was however later discovered that the effects mediated by the RNAi were due to an off-target effect, which we've yet to identify. Transcriptional analysis of *abrupt*-RNAi (KK) expressing cells showed that Xrp1, an established mediator of cell competition, was highly upregulated. This suggests that the *abrupt*-RNAi (KK) line may drive cell competition through upregulation of Xrp1. Overexpression of the "long" isoform of Xrp1($Xrp1^{Long}$) caused chronic activation of stress pathways and rapid cell death while the "Short" isoform ($Xrp1^{Short}$) had no effect, suggesting the competitive function of Xrp1 may be isoform dependent. Inhibition of the Nrf2-kinase PERK, alleviated loser cells from UPR signalling, but did not rescue them from Nrf2 activation.

Author’s declaration

I declare that the work in this dissertation was carried out in accordance with the requirements of the University's Regulations and Code of Practice for Research Degree Programmes and that it has not been submitted for any other academic award. Except where indicated by specific reference in the text, the work is the candidate's own work. Work done in collaboration with, or with the assistance of, others, is indicated as such. Any views expressed in the dissertation are those of the author.

SIGNED: ..... DATE:.....

Acknowledgements

I would like to begin by thanking Eugenia Piddini for accepting me into her wonderful lab. It has been an absolutely pleasure working with her, and very educational. Her unwavering optimism helped drive me through my project and I'm inspired by her ability to approach problems from multiple angles. My time in the Piddini lab, albeit shorter than I had hoped, has given me invaluable insight into the world of research which will stay with me throughout my career.

Another pillar in this project is Paul Langton, who designed and oversaw my experiments every day. Providing continuous support and insight throughout the project, Paul has been crucial in everything presented in this thesis. His knowledge when it comes to *Drosophila* is second to none, and I am extremely grateful for being able to learn from him about the wonders of flies.

I also want to thank my good friends and fellow lab mates Michael Baumgartner and Alex Mastrogiannopoulos both for help in the lab as well as showing me around the great city of Bristol, my time in Bristol would have been much lonelier without them. The macro developed by Michael also played a pivotal role in this project, saving me an immense amount of time which would otherwise be spent on quantifications. Also, many thanks to Remi Logeay for assisting me with things related to transcriptional analysis.

I also want to thank all the members of Piddini lab and Salas lab, for being an absolute joy to work with! I want to thank Parthive Patel and Sam Huguet for many interesting conversations. Also special thanks to Kelly for keeping the lab running like a well-oiled engine, and for helping me with all things lab related. My time in the lab would have been much different without the wonderful set of individuals gathered there.

A special thanks to the University of Bristol and to the staff of the department of Cellular and Molecular medicine, for accommodating me and helping me throughout my project.

Finally, I would like to thank my family for their constant support and encouragement.

Abbreviations

ab	*abrupt*
act	actin promoter sequence
ago2	*argonaute 2*
ATF4	Activating transcription factor 4
Bip	Binding immunoglobulin protein
Br140	Bromodomain-containing protein, 140KD
BSA	Bovine serum albumin
bsk	*basket* (*Drosophila* homologue of JNK)
bst	Belly spot and tail
BTB	Broad-Complex, Tramtrack, Bric-a-brac
bZIP	Basic leucine zipper
CHOP	C/EBP-homologous protein
Ct	Cycle threshold value
dDNA	Genomic DNA
dMyc	*Drosophila* homologue of *Myc*
DSB	Double-Strand Break
eIF2α	α subunit of eukaryotic translation initiation factor 2
en	*engrailed*
ER	Endoplasmic reticulum
ESC	embryonic stem cell
EV	Empty vector
FBS	Fetal bovine serum
FK2	Antibody for polyubiquitinated proteins
FLP	Flippase recombinase
FRT	Flippase recognition target
GADD	Growth arrest and DNA damage-inducible protein 34
GAL4	Transcription factor which binds to UAS
GAL80TS	Temperature sensitive GAL80
GFP	Green fluorescent protein
GSTD1	Glutathione S-Transferase
GSK-3β	Glycogen Synthase Kinase 3β
HA	Haemagglutinin
hh	hedgehog
hh-flp	*hedgehog-flippase* construct
IRBP	Inverted Repeat Binding Protein
IRBP 18	Inverted Repeat Binding Protein 18 kDa
ISR	Integrated Stress Response
JAK	Janus Kinase
JNK	C-Jun N-terminal Kinase
M	*Minute*
MARGE	Mutant analysis by rescue gene excision Flp-out system
Minute	Ribosomal gene mutations
MiWo	*Minute* in Wild type organism
Myc	transcription factor and Proto-oncogene
NFkB	Nuclear factor kappa-light-chain-enhancer of activated B cells
NMD	Nonsense Mediated mRNA decay
Nrf2	Nuclear factor erythroid 2-related factor

OPP	O-propargyl-puromycin
PBS	Phosphate buffered saline
p-eIF2α	phosphorylated-eIF2α
PERK	ER-associated protein kinase
PFA	paraformaldehyde
p-JNK	phosphorylated-JNK
qPCR	Quantitative PCR/Real-time PCR
RIDD	Regulated Ire1-dependent decay
RNAi	RNA interference
RPs	Ribosomal proteins
RpS3	Ribosomal protein Subunit 3
RT	Room temperature (21 °C)
scrib	*scribbled*
STAT	Signal Transducer and Activator of Transcription
TIRs	Terminal inverted repeats
UAS	Upstream Activation/Activating Sequences
UPR	Unfolded protein response
WT	Wild Type
Xrp1^{HA}	Haemagglutinin-tagged Xrp1^{Long}
Xrp1^{Long}	Long isoform of Xrp1
Xrp1^{Short}	Short isoform of Xrp1

Table of Contents

Abstract i
Author's declaration ii
Acknowledgements iii
Abbreviations iv
1 Introduction 1
1.1 The principles of cell competition 1
1.1.1 *Minute* mutations 1
1.2 Defining a loser 5
1.2.1 The loser signature 5
1.2.2 Nrf2 targeted screening 8
2 Aims and objectives 12
3 Methods 13
3.1 Fly maintenance 13
3.1.1 General maintenance 13
3.1.2 *Minute* clone induction 14
3.1.3 Mitotic recombination 15
3.1.4 Genotype list 17
3.2 Fluorescencent staining 18
3.2.1 Antibody staining 18
3.2.2 Translation assay (OPP) 19
3.2.3 List of Antibodies 19
3.3 Image acquisition and analysis 21
3.4 DNA extraction and PCR 21
3.5 RNA extraction 22
3.5.1 RNA extraction using separation columns 22
3.5.2 RNA extraction using Trizol reagent 23
3.6 Reverse transcription 24
3.6.1 DNase treatment 24
3.6.2 Reverse transcription 24
3.7 Quantitative Real-Time PCR (qPCR) 25
3.8 Statistics 26
3.8.1 Confocal 26
3.8.2 Quantitative Polymerase chain reaction (qPCR) 26
4 Investigating the function of Abrupt in cell competition 27
4.1 Rationale 27

4.2 Results 28
4.2.1 The *abrupt*-RNAi (KK) line enhances cell competition 28
4.2.2 Xrp1 inhibition rescues *abrupt*-RNAi loser phenotype 33
4.2.3 Identifying off targets of *abrupt*-RNAi 34
4.3 Discussion 42
4.4 Conclusion 46
5 Investigating the consequences of Xrp1 overexpression 47
5.1 Rationale 47
5.2 Results 48
5.2.1 The function of Xrp1 in cell competition is isoform dependent 48
5.2.2 Inhibition of Irbp18 mildly rescues *Minutes* from stress 52
5.3 Discussion 54
5.4 Conclusion 56
6 PERK inhibition 57
6.1 Rationale 57
6.2 Results 58
6.3 Discussion 61
6.4 Conclusion 63
7 General discussion 64
8 References 66

Figures

Figure 1: Schematic representation of classical (Minute) cell competition and super-competition. 3
Figure 2: Defining a loser cell 6
Figure 3: Loser cells suffer from enhanced proteotoxic stress 9
Figure 4: Schematic representation of the MiWo tool. 15
Figure 5: Schematic for mitotic recombination. 16
Figure 6: abrupt-RNAi (KK) line enhances competition. 28
Figure 7:The effect of abrupt-RNAi (KK) line effect on oxidative stress pathway and translation. 30
Figure 8: p-eIF2α and Xrp1 are elevated in abrupt-RNAi (KK) cells. 32
Figure 9: Inhibition of Xrp1 in abrupt-RNAi clones in a WT background rescues them from elimination. 33
Figure 10: Abrupt mutant (Abrupt^{P}) clones do not affect cell death or stress pathway activation. 35
Figure 11: Abrupt mutant clones do not display enhanced border cell elimination. 36
Figure 12: The abrupt-RNAi (KK) line does not target abrupt but causes a stong upregulation of Xrp1. 39
Figure 13: Inhibition of abrupt causes a mild upregulation in oxidative stress pathway activation and factors involved in the UPR. 41
Figure 14: The competitive function of Xrp1 is isoform dependent 49
Figure 15: Overexpression of the Xrp1^{Long} isoform causes an accumulation of misfolded proteins and enhances UPR signaling. 50
Figure 16: Overexpression of Xrp1 tagged with HA (Xrp1-HA) triggers the oxidative stress response and drives cell death. 51
Figure 17: Inhibition of Irbp18 causes a mild rescue of the oxidative stress response pathways and Unfolded protein response in Minutes. 53
Figure 18: PERK inhibtion rescues RpS3$^{+/-}$ cells from hyperactivation of the UPR but has no significant effect on the oxidative stress response. 59
Figure 19: Inhibition of PERK does not affect cell death in Minute discs, but shows a trend towards elevated JNK activation. 60
Figure 20: Proposed model for how abrupt-RNAi (KK) line confers the loser status. 65

Tables

Table 1:Genotype list 17
Table 2: List of primary antibodies 19
Table 3: List of secondary antibodies 20
Table 4: Oligonucleotides used in this project. 25

1 Introduction

1.1 The principles of cell competition

1.1.1 *Minute* mutations

In early development, a small number of cells serve as the precursors to all tissues of the body. If only a few of these cells are aberrant, their continued proliferation may compromise the entire organism. Retention of tissue homeostasis is therefore critical for healthy development of an individual, where all multicellular organisms have in place intrinsic mechanisms for the removal of unwanted cells in order to maintain a healthy tissue (Biteau et al., 2011). Although autonomous apoptotic mechanisms are well understood, there exists another less characterized process called cell competition. Cell competition is a process where cells achieve tissue homogeneity by continuously comparing themselves to each other through various mechanisms whereby less-fit "loser" cells are eliminated by fitter "winner" cells (Clavería et al., 2013, Wagstaff et al., 2016).

Cell competition was first discovered by Ripoll and Morata in 1975 while investigating mutations of the Ribosomal Proteins (RPs) in the larval wing discs of the fruit fly: *Drosophila melanogaster* (Morata and Ripoll, 1975). This group of RP mutations were named *Minute*, due to the characteristically small bristle size and reduced growth of flies heterozygous for the mutation (*M*/+) (Bridges and Morgan, 1923). While heterozygous viable, most *Minute* mutations proved homozygous cell lethal as all ribosomal components are required for its function (Marygold et al., 2007). While investigating this group of mutations they found that although *M*/+ cells are viable in a homogenous tissue, when clonally generated in a WT background *M*/+ clones grew much smaller than other non-*Minute* clones induced in a similar fashion. Furthermore, when WT clones were generated in a *Minute* tissue, they grew considerably larger (Morata and Ripoll, 1975). Similar behaviour could also be observed when *Minute* cells with differing mitotic rates were co-cultured (Morata and Ripoll, 1975, Simpson and Morata, 1981). It was later found that the reduced size of *Minute* clones was caused by elimination by their fitter WT neighbours (Figure 1), driven by caspase dependent apoptosis (Moreno et al., 2002). Together these discoveries laid the foundation for the subject of cell competition, where ribosomal mutations have served as a frequent model for loser cells.

Although initially discovered in flies, similar behaviour was later discovered in mammals, where mouse cells heterozygous for mutated forms of the ribosomal protein gene: Belly spot and tail (*bst*) were eliminated by their WT neighbours (Oliver et al., 2004). Furthermore, recent studies of the Wnt/β-catenin morphogen gradient in zebrafish (*Danio rerio*) embryos hint that cell competition also functions to correct noise in signalling gradient systems during embryogenesis, indicating that cell competition may serve a more diverse role in development (Akieda et al., 2019).

In the classical model for cell competition described by Ripoll and Morata, WT cells always outcompete aberrant cells such as *Minutes*, this however is not always the case as certain factors have been found to give cells a competitive advantage, causing them to eliminate surrounding WT cells (Morata and Ripoll, 1975). This was discovered during investigation of *Myc*, a transcription factor which regulates growth through modulation of *de novo* ribosome biogenesis (Grewal et al., 2005). Reduced expression of the *Drosophila* homologue of *Myc* (*dMyc*) in clones, caused them to be eliminated in a similar fashion as *Minute* cells (Johnston et al., 1999, Moreno et al., 2002). However, overexpression of *Myc* reverses the roles, where *Myc* overexpressing clones eliminate surrounding WT cells at the expense of the host tissue (de la Cova et al., 2004, Moreno and Basler, 2004). This form of cell competition where aberrant cells outcompete their host was later named super-competition (Figure 1) and has been demonstrated to occur in several cancer models (Moreno and Basler, 2004, Suijkerbuijk et al., 2016).

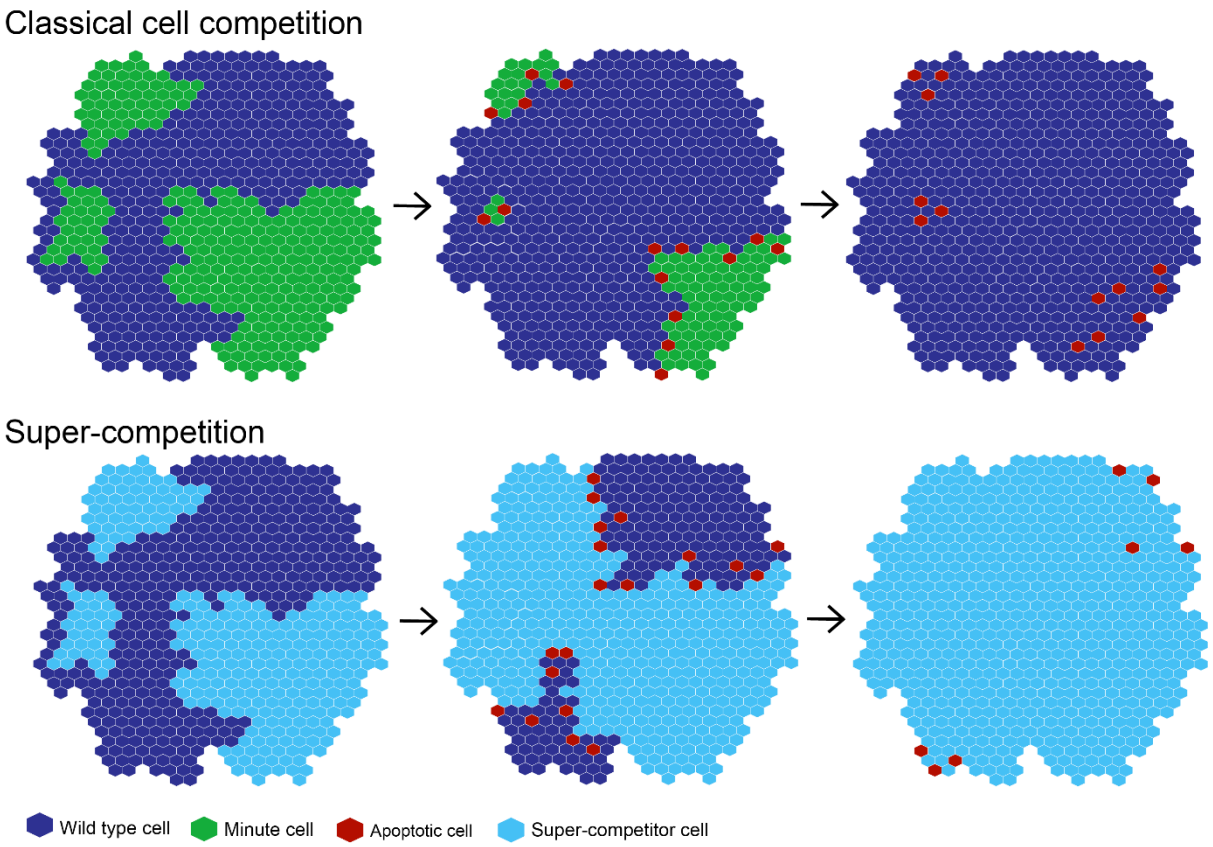

Figure 1: Schematic representation of classical (*Minute*) cell competition and super-competition.

In classical cell competition less fit *Minute* cells (Green) are eliminated by surrounding wild type (WT) cells (Dark blue) by driving them to apoptosis (Red). Ultimately tissue homeostasis is restored with WT cells overtaking the tissue. In super-competition, the opposite occurs where the super-competing cells (light blue) outcompete host WT cells, eventually overtaking the entire tissue.

Much like classical competition, super-competition was found to occur in mammals, where in mouse (*Mus musculus*) early embryos, relative *Myc* expression serves as a determinant of embryonic stem cell (ESC) fitness (Sancho et al., 2013). In early mouse development, prior to gastrulation, cells in the inner cell mass of the mouse blastocyst are highly sensitive to DNA-damage and large peaks in apoptotic cells occur in the primitive streak of the developing embryo (Manova et al., 1998, Heyer et al., 2000). This suggested that cellular fitness was tightly regulated during these stages of development where heterogeneity in *Myc* expression in a tissue is cleared through elimination of low-*Myc* cells by neighbouring high-*Myc* cells (Clavería et al., 2013, Díaz-Díaz et al., 2017). After this pioneering discovery, several other growth factor signalling pathways were found to drive cells to become super-competitors, this includes the JAK-STAT, Hippo and Wnt signalling pathways, many of which are heavily implicated in cancer (Moreno and Basler, 2004, Neto-Silva et al., 2010, Rodrigues et al., 2012, Suijkerbuijk et al., 2016, Madan et al., 2019). This sparked the idea of super-competition serving a role in cancer as a means for oncogenic cells to clear new niches for them to expand through elimination of their neighbours. Investigation of competitive cancer models in both flies and mammals supported this theory where inhibition of cell engulfment mechanisms in tumours arrested their expansion through the host tissue (Eichenlaub et al., 2016). Furthermore, expansion of $APC^{-/-}$ adenomas in *Drosophila* can be blocked by inhibiting apoptosis in the organism, rendering the tumours indistinguishable from wild type (Suijkerbuijk et al., 2016). The fact that tumour expansion can be halted by inhibiting competition yields exciting prospects for potential therapeutic methods against cancer (Vishwakarma and Piddini, 2020).

1.2 Defining a loser

1.2.1 The loser signature

Despite accumulating discoveries of mutations that cause cell competition, the mechanisms which drive cells to become winners or losers remain elusive. To determine what drives cells to become winners and losers, it is important to understand the state of cells prior to competition. Winners and losers are only determined when confronted by each other, but before competitive interaction occurs, they are termed as prospective winners and prospective losers, respectively. In this context *Minute* mutations fall into the category of prospective loser mutations as *Minute* cells are viable in a homotypic environment.

In a recent study performed by our lab, transcriptional analysis of *Drosophila* homotypic tissues of various prospective loser mutations was performed in order to determine which genes are differentially expressed in prospective loser mutants (Kucinski et al., 2017). In this case the transcriptome *RpS3* and *Mahjong* mutant wing discs along with separate *Rps15* mutations, which cause a *Minute* phenotype but do not behave as a loser, were compared to WT cells. Two distinct mutated alleles for *RpS3* were investigated (*RpS3* and *RpS3**) (Kucinski et al., 2017). Interestingly, despite the *RpS3* and *RpS15* being functionally related, the transcriptome of the two *RpS3* mutants had more in common with the *Mahjong* mutants than the *RpS15* mutants (Figure 2). This indicated that there is a common shared molecular signature in prospective loser cells which may be indicative of a similarity in their cellular state (Kucinski et al., 2017). Later investigation into the shared molecular signature of the prospective loser phenotypes revealed that several genes encoding components of signalling pathways were differentially regulated, and factors involved in the cellular stress response, DNA repair and oxidative-reduction were highly enriched (Kucinski et al., 2017). The Toll signalling, P53/DDR, JAK/STAT, JUN N- terminal kinase (JNK) (*Basket* (*Bsk*) in *Drosophila*) and the oxidative stress response pathways were among the signalling pathways implicated in the loser signature all of which now have established function in various processes in cell competition (Kucinski et al., 2017). Subsequently, several factors involved in the Unfolded Protein Response (UPR) were later also found to be affected in *Minute* cells, including the Eukaryotic Translation Initiation Factor 2 α (eIF2α) which has been shown to be highly activated in *Minutes*, (Figure 2) (Dinan, 2018).

The tumour suppressor P53 is known to drive hypersensitivity to cell crowding and regulate homeostatic cell density in another form of cell competition known as mechanical cell competition (Wagstaff et al., 2016). Unlike older models for cell competition which are based on mechanisms involving molecular exchange, mechanical cell competition refers to the ability of cells to be eliminated by their neighbours through mechanical insults such as compaction (Wagstaff et al., 2016, Matamoro-Vidal and Levayer, 2019). Differential P53 activity is also capable of driving competition in mouse ESCs (Zhang et al., 2017) as well as in hematopoietic stem cell niches (Marusyk et al., 2010).

Activation of JNK signalling, which occurs downstream of ER-stress (Figure 3), is common among different loser types, including *Minute* cells (Figure 2) where it is thought to inhibit their growth and expansion in the host tissue (Kucinski et al., 2017, Pérez et al., 2017, Pinal et al., 2019). Although JNK signalling negatively regulates growth of losers it also serves a contradictory function in winner cells where, in certain tumour models it promotes growth of super-competitors through mitogenic signalling (Igaki et al., 2006). The JAK/STAT pathway is frequently activated in human cancers (Groner and von Manstein, 2017) and has been shown to enhance proliferation of winner cells in *Drosophila* (Rodrigues et al., 2012, Kucinski et al., 2017).

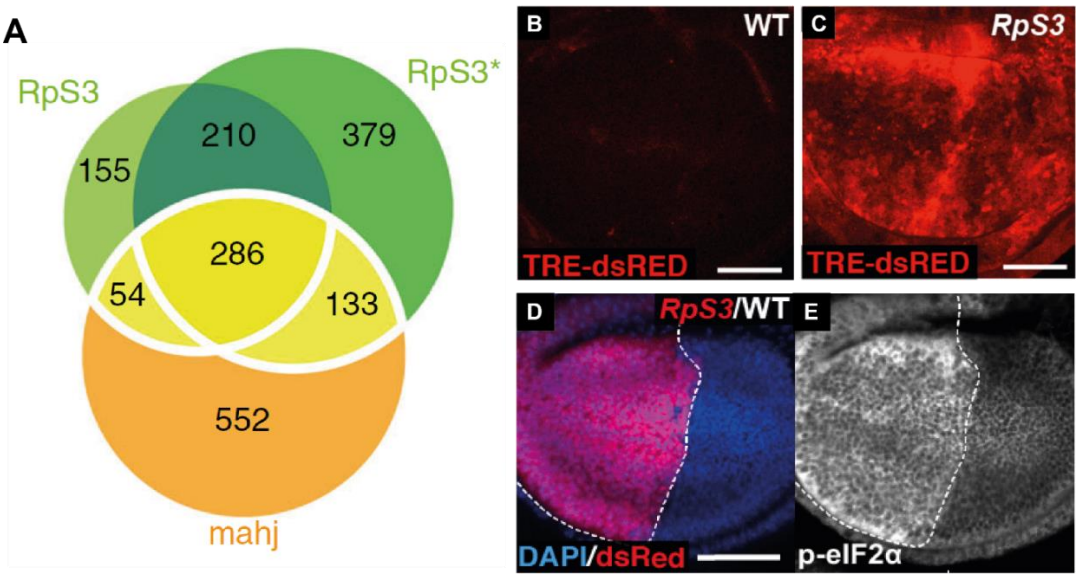

Figure 2: Defining a loser cell

(A)Venn diagram representing genes commonly differentially expressed in the prospective loser genotypes: RpS3 and RpS3* (two distinct mutant alleles for *RpS3*) and Mahjong, figure from (Kucinski et al., 2017). (B & C) JNK signalling in a homogenous $RpS3^{+/-}$ mutant wing disc in comparison to a wild type wing disc measured with a TRE-dsRED marker (Kucinski et al., 2017). D, E) Wing disc with a $RpS3^{+/-}$ anterior compartment (marked with dsRED), and wild type posterior compartment, stained for phosphorylated eIF2α (p-eIF2α) (Dinan, 2018).

Both the JAK/STAT and JNK pathways are regulated by Xrp1, a transcription factor carrying a Basic Leucine Zipper (*bZIP*) domain and AT-hook domain which is activated downstream P53 in response to UV irradiation (Brodsky et al., 2004, Baillon et al., 2018, Blanco et al., 2020). Xrp1 is also plays a critical role in competition, contributing to over 80 % of gene expression changes in *Minute* loser cells (Lee et al., 2018). Upregulation of *Xrp1* is common among the majority of loser types, where it drives the loser status through regulation of various processes influencing translation and growth (Lee et al., 2018). The critical importance of Xrp1 in cell competition was established with the discovery that its knockdown is sufficient to rescue most loser cells from competitive elimination by their neighbours (Kale et al., 2015, Lee et al., 2018, Baker et al., 2019, Blanco et al., 2020). Furthermore knockout of Xrp1 in *Minute* cells improved their growth rate considerably (Lee et al., 2018) Xrp1 is a component of the larger Inverted Repeat Binding Protein (IRBP) complex, where it forms a heterodimer with another protein called Irbp18 (Francis et al., 2016). The Irbp18/Xrp1 heterodimer has high binding affinity to P-element 31-bp terminal inverted repeats (TIRs), located on opposite ends of P-transposable elements which serve an important role in transposase cleavage. With its specific binding to TIRs, the Irbp18/Xrp1 heterodimer functions within the IRBP complex in repair of Double-Strand Breaks (DSB) in response to transposase cleavage (Francis et al., 2016).

The function of Xrp1 in competition has been shown to be dependent on Irbp18, where its knockout, similar to inhibition of Xrp1, rescues loser cells from competition (Blanco et al., 2020). While Irbp18 is Xrp1s only known binding partner (Reinke et al., 2013), Irbp18 also interacts with ATF4, a factor involved in proteotoxic stress response pathways (Blanco et al., 2020). Unlike Irbp18 however, ATF4 does not rescue loser cells from elimination indicating that the competitive effects mediated by Irbp18 occurs primarily through the Irbp18/Xrp1 complex (Blanco et al., 2020).

1.2.2 Nrf2 targeted screening

Further investigation into genes implicated in the loser signature (Figure 2) revealed that the majority of genes involved in the oxidative stress response were regulated by the transcription factor: Nuclear Factor erythroid 2-Related Factor 2 (Nrf2) (CncC in *Drosophila*) which is chronically activated in *Minutes* (Sykiotis and Bohmann, 2008, Kucinski et al., 2017). Clonal overexpression of Nrf2 is sufficient to turn WT cells into losers, indicating that Nrf2 is a major driver of cell competition (Kucinski et al., 2017). It can also be noted that oxidative damage does not contribute to the ability of Nrf2 to mediate the loser status, suggesting that the oxidative stress signalling is what drives cells to become losers not perturbations incurred by oxidative damage (Kucinski et al., 2017). Activation of Nrf2 is mediated by the endoplasmic reticulum (ER) membrane-bound PKR-like endoplasmic reticulum kinase (PERK) in response ER-stress (Figure 3) (Cullinan and Diehl, 2006). PERK also acts as a kinase for eIF2α, which when phosphorylated (p-eIF2α) shuts down global translation (Figure 3) (Pakos-Zebrucka et al., 2016). As a part of the UPR pathway, PERK is activated by Binding immunoglobulin protein (Bip), an ER-localized chaperone, in response to accumulation of misfolded proteins (Hetz et al., 2011). Increased p-eIF2α and repressed global translation are common in *Minute* losers (Figure 3) and translational efficiency has long been considered among the primary determinants of cellular fitness in *Minutes* (Moreno et al., 2002). However

In the loser specific molecular signature, PERK is upregulated as well as another eIF2α kinase: GCN2, which is activated downstream amino acid deprivation and glucose starvation (Figure 3) (Ye et al., 2010). In addition to shutting down global translation, p-eIF2α also causes selective translational upregulation of ATF4 which in turn enhances pro-survival signalling pathways (Figure 3). While ATF4 is capable of promoting cell viability for a limited time, in instances of extended ER-stress such as in *Minute* cells, ATF4 adopts a pro-apoptotic role instead (Kim et al., 2008).

ATF4 is also a transcription factor which mediates expression of C/EBP-homologous protein (CHOP), which activates pro-apoptotic genes. CHOP activates Growth arrest and DNA damage-inducible protein (Gadd34) (Hetz et al., 2011), which acts as a eIF2α phosphatase, forming a negative feedback loop for unfolded protein response (UPR) (Figure 3) (Hetz et al., 2011). Research performed by a previous PhD student in our lab showed that inhibition of Gadd34 via RNAi caused an increase in eIF2α activation and attenuation of global translation in *Drosophila* tissues. The inhibition of Gadd34 also caused an increase in Nrf2 activation which was sufficient to drive cells to become losers, further supporting that accumulation of misfolded proteins and ER-stress drives Nrf2 expression in losers (Dinan, 2018).

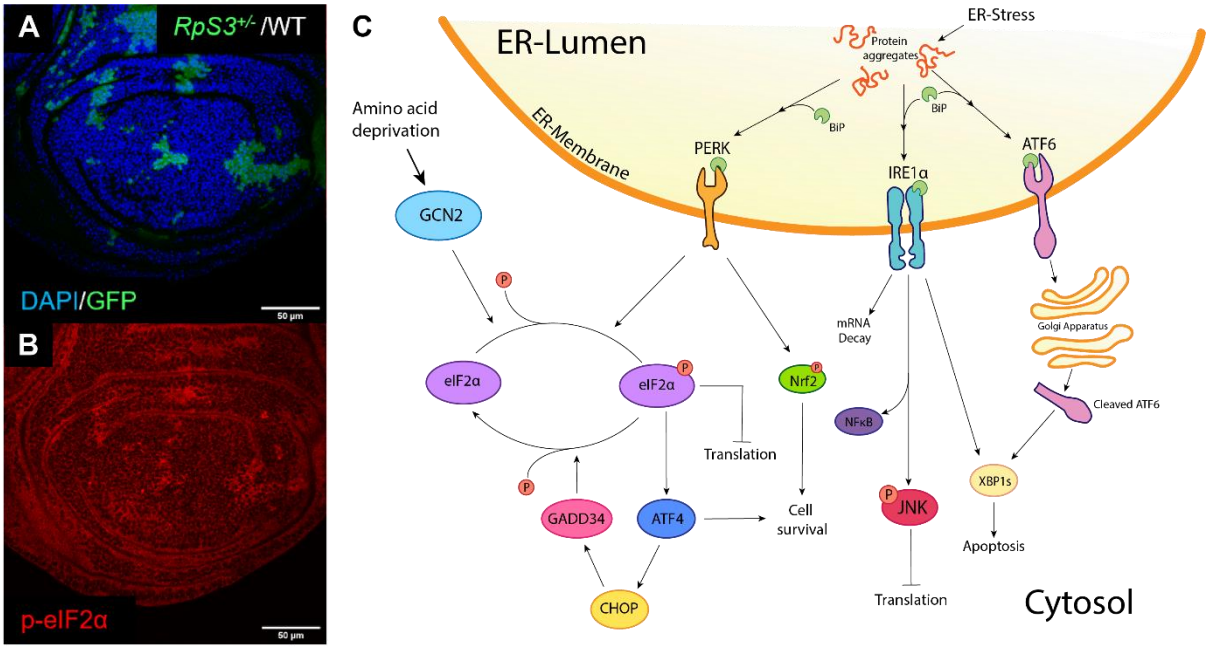

Figure 3: Loser cells suffer from enhanced proteotoxic stress

(A- B) Wild type (WT) clones mitotically generated in a GFP expressing *RpS3*$^{+/-}$ *Drosophila* wing disc (green) with and antibody stained for phosphorylated eiIF2α (p-eIF2α) (Red). Images from Anna Takeuchi (Takeuchi, 2019). (C) Schematic representation of the Unfolded protein response (UPR) in mammals, figure adapted from schematics by Michael Dinan and Claudio Hetz (Dinan, 2018, Hetz et al., 2011).

In order to determine how Nrf2 mediates its competitive function, downstream effectors of Nrf2 in cell competition were investigated by members of our lab. Comparison of the transcriptional profile of Nrf2 overexpressing cells to the loser signature showed a considerable overlap, with 121 genes shared between the two groups. These genes were further investigated in a genetic screen, where they were downregulated via RNAi in *Minute* loser clones generated in a *Drosophila* wing disc using the MiWo tool (see methods chapter 3.1.2). Measuring how the inhibition of Nrf2 target genes influences the rate of elimination of the loser clones provided a simple yet effective method to determine whether the genes were involved in cell competition or not. If the inhibition of a target gene lead to a reduced rate of elimination, thus larger clones, it indicated that the target gene enhances loser cell elimination. In contrast if inhibition of a gene enhances rate of elimination, resulting in diminished loser clone size, the gene functionally reduces loser cell elimination. If the rate of elimination and clone size remained unchanged then it could be concluded that either the gene did not play a direct role in competition, or that the RNAi was not functional.

Among the *Nrf2* target genes which showed the most pronounced phenotype was the transcription factor *abrupt*. Inhibition of *abrupt* in loser clones caused them to be eliminated at a rapid rate, leaving very small clones behind. This prompted us to further investigate the role of *abrupt* in cell competition. Relatively little is known about *abrupt* in the context of cell competition, it encodes a Broad-Complex, Tramtrack, Bric-a-brac (BTB)-domain-zinc Finger transcription factor which plays a diverse role in various developmental processes including ovarian cell migration, dendritic morphogenesis, epithelial development of imaginal discs and more (Turkel et al., 2013). Reduced expression of *abrupt* in *Drosophila* causes the *abrupt*-vein phenotype which is characterized by impaired development of the L5 vein of the fly wing causing a shortened vein or a lack of L5 vein altogether. The BTB-domain Zinc Finger transcription factors are a large protein family, containing multiple human proteins involved in cancer (Costoya, 2007, Kelly and Daniel, 2006). Although not capable of promoting tumour growth in *Drosophila* tissues when overexpressed on its own, *abrupt* has been shown to form massive tumours when overexpressed in the eye/antennal disc carrying a loss of function mutation of the cell polarity factor *scribbled* (*scrib*), with said tumours retaining a progenitor-like state through inhibition of multiple regulators of cell fate (Turkel et al., 2013). Furthermore, considerable enrichment of binding sites associated with both JNK and Toll signalling pathways could be observed in *abrupt* overexpressing *scrib* mutant tumours, which suggests both pathways are involved in the tumorigenic cooperation of *abrupt* and *scribbled*.

Interestingly, *scribbled* is well established in the field of cell competition, where *scrib* deficient cells have been shown to be eliminated by WT cells in a JNK dependent manner (Norman et al., 2012). Given its close relation with factors involved in cell competition, *abrupt* showed promise as a potential novel mediator of cell competition.

2 Aims and objectives

In this project, we investigated genes identified in a candidate-based screen to determine whether they play a role in the process of cell competition. Among the genes identified in the screen was the gene *abrupt* which showed a promising competitive phenotype in the screen and is known to interact genetically with factors with established roles in cell competition. Furthermore, we also pursued other factors involved in competition, including Xrp1 and members of the PERK branch of the UPR, and their relation to stress pathway activation. The *Drosophila* wing disc was used as a model, with which we were able to carry out various competitive assays. The versatility of *Drosophila* genetics allowed us to probe candidate genes in multiple ways to determine how different genetic perturbations influence the competitive fitness of the cells. By pursuing these candidate genes, we hoped to discover novel mediators of competition, which would help us further understand what drives cells to compete. Understanding how competition works may provide invaluable insight into how tumours proliferate, potentially laying the foundation for the development of treatments.

This project could therefore be broken up in to 3 separate projects, all pursuing different pathways of cell competition:

A. Investigate the transcription factor Abrupt, in the context of cell competition.
    1. Measure whether Abrupt inhibition via RNAi is sufficient to drive cells to compete.
    2. Understand how Abrupt influences established markers of the loser status such as eIF2α, Nrf2, JNK.
    3. See whether phenotype can be produced via mutant alleles.
    4. Measure whether Abrupt regulates Xrp1 expression.

B. Determine the contribution of Xrp1 to the loser phenotype.
    1. Establish conditions for Xrp1 overexpression to emulate levels observed in Minute loser phenotypes.
    2. Characterize Xrp1 overexpression with respect to loser-state read-outs.
    3. Measure whether Irbp18 inhibition is sufficient to rescue cells from the loser status.

C. Measure the role of the UPR in cell competition.
    1. Evaluate the contribution of the unfolded protein response to the loser status by inhibiting PERK.
    2. Assess how PERK inhibition affects loser-state read-outs.
    3. Measure whether PERK inhibition rescues loser cells from being eliminated by WT cells.

3 Methods

3.1 Fly maintenance

3.1.1 General maintenance

Fly stocks were maintained at room temperature in standard wheat-based fly food composed of 7.5 g l^{-1} agar powder, 50g l^{-1} baker's yeast, 55 g l^{-1} wheat flour, 2.5 % nipagin, 1 % penicillin/streptomycin and 0.4 % propionic acid. Each new fly stock was checked for mites prior to experimental use. Experimental crosses were maintained in a 25 °C incubator unless otherwise indicated. For temperature-sensitive experiments, such as $GAL80^{ts}$ crosses and heat shocks, heated water baths were used. Expression of genes under $GAL80^{ts}$ can be regulated by incubating at specific temperatures where at 18°C $GAL80^{ts}$ is functional and capable of inhibiting GAL4 based drivers (and thus their downstream genes), but at temperatures above 29°C it becomes inactive, thus allowing GAL4 to activate. For most experiments, several independent crosses were maintained in separate tubes in identical conditions where technical replicates were collected from each tube over a period of several days. All organisation of experiments and genetic designs were overseen by Paul Langton.

3.1.2 *Minute* clone induction

For the generation of *Minute* clones in a phenotypically wild type background we used the *Minute* in Wild type organism (MiWo) tool, developed by a previous member of our lab (Dinan, 2018). The MiWo tool is based on Mutant analysis by rescue gene excision (MARGE), an approach in which mutant cells are generated through a loss of a rescue transgene (Zhou et al., 2016). The MiWo tool chromosome contains two copies of *RpS3*: one mutant *RpS3* ($RpS3^{Plac92}$) copy and a construct containing a rescuing *RpS3* transgene flanked by Flippase recognition target (FRT) sites with a downstream GAL4 coding sequence (Figure 4). An upstream actin promoter maintains *RpS3* transgene expression at levels which rescues them from the *Minute* phenotype, making them phenotypically wild type cells. Clone induction was achieved through the expression of Flippase (FLP) recombinase, whose transcription is dependent on a heat-shock promoter which is activated at 37 °C. When FLP is expressed it excises the rescuing *RpS3* transgene flanked by FRT sites, turning cells *Minute*, and leaving behind a single FRT site. This recombination event moves the GAL4 encoding sequence under the influence of the actin (*act*) promoter causing GAL4 to be transcribed. The expressed GAL4 binds to and activates the Upstream Activation Sequence (UAS) enhancer causing an additional UAS-*GFP* transgene to be expressed, thus labelling *Minute* clones with GFP. In addition to GFP, other constructs such as RNAis can be placed downstream of the UAS in order to specifically express them in *Minute* clones. This allows us to monitor how the expression of various genes influences cell competition between the GFP expressing *Minute* clones and neighbouring phenotypically WT cells.

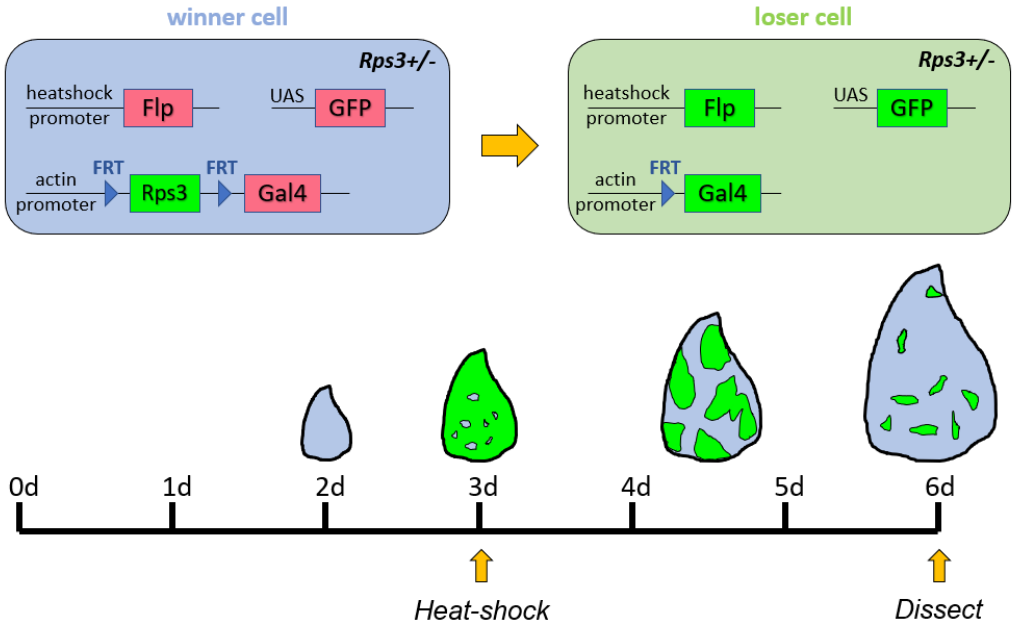

Figure 4: Schematic representation of the MiWo tool.

Phenotypically WT cells containing the MiWo construct and a Flippase (*Flp*) encoding cassette downstream a Heat-shock promoter (expressed coding sequences shown in green, and non-expressing indicated with red). Downstream of an actin promoter, a rescuing Ribosomal Protein Subunit 3 (*RpS3*) gene is flanked by *FRT*-sites and followed by a GAL4 encoding sequence. Larvae are heat-shocked (37 °C) on day 3 after initial eggs were laid. This activates the heat-shock promoter, driving FLP expression which causes a recombination event between the *FRT* sites, excising the rescuing *RpS3* gene, turning cells *Minute*. The excision also places the *GAL4* sequence under the influence of the actin promoter (*act*) causing it to be expressed. GAL4 in turn activates the UAS promoter causing downstream GFP to express, thus labelling recombined $RpS3^{+/-}$ cells. The MiWo tool can be paired with an UAS driven RNAi line to downregulate specific genes in MiWo generated *Minute* clones.

3.1.3 Mitotic recombination

For the generation of non-*Minute* clones, a FLP/FRT-based genetic mosaic system was used. This method utilizes FLP dependent mitotic recombination between FRT sites, located close to the centromeres, for the generation of homozygous clones in a heterozygous background, recombination was initiated during development with a 37 °C heat shock which activates a heat shock promoter which drives FLP expression. In a cell heterozygous for a marker gene, mitotic recombination would yield two clones, called twin spots, one homozygous for the marker and one without. By placing a mutation distal to the FRT site on one arm of a homologous chromosome and a marker on the other it allows for the labelling of mutant clones based on the number of marker copies expressed (Figure 5) (Lee, 2014, Xu et al., 2019).

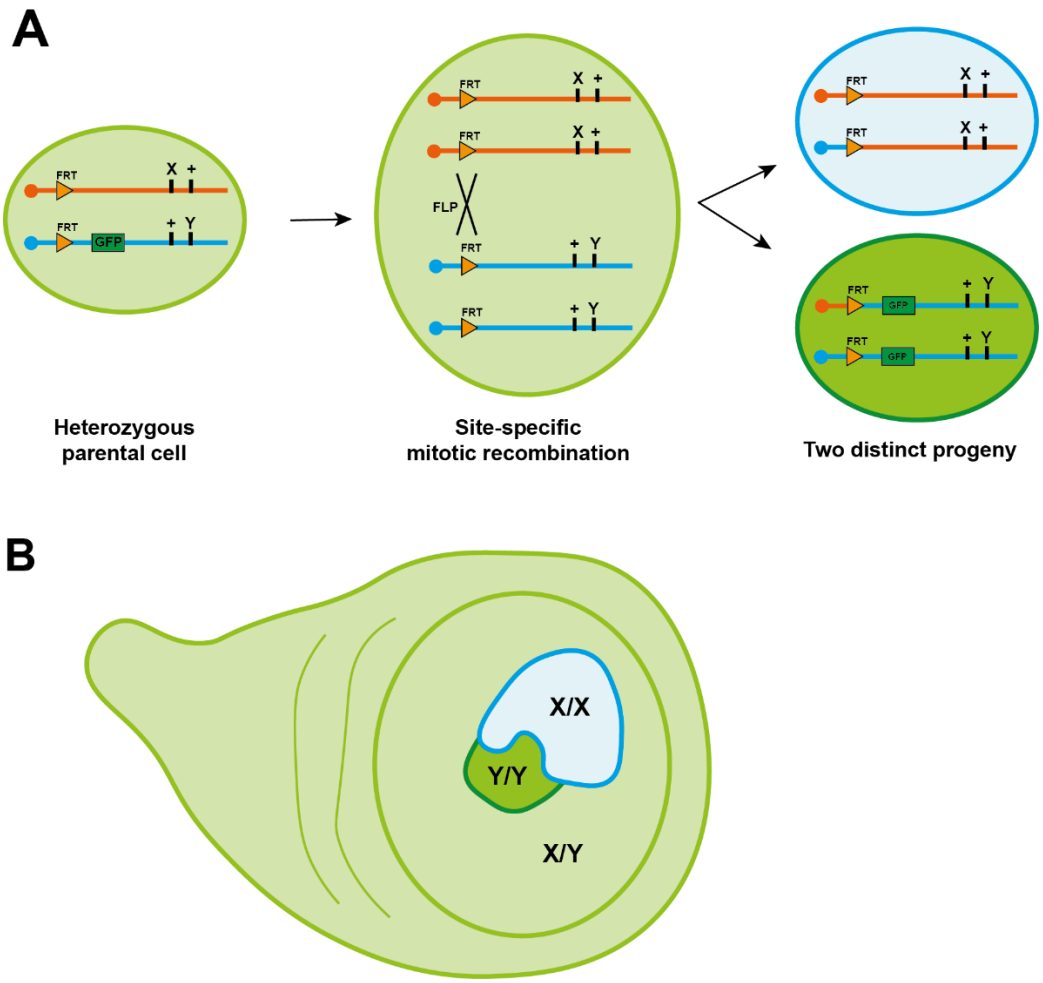

Figure 5: Schematic for mitotic recombination.

Adapted from schematic presented by Lee and colleagues (Lee, 2014). (A) Two distinct daughter-cells can emerge from a single parental cell following mitotic recombination. This occurs through the FLP/FRT based recombination system, where a Flippase (FLP) drives recombination between FRT sites (Orange triangles), producing cells with different alleles and transgenes distal to the recombination site. (B) Schematic of a heterozygous wing disc (Light green), carrying the two distinct and adjacent homozygous X/X (Light blue) and Y/Y (Green) clones generated via mitotic recombination

3.1.4 Genotype list

Below is the list of genotypes of larvae dissected for experiments represented in figures.

Table 1: Genotype list

Figure panel	Genotype
Figure 6	$\frac{hs-Flp, UAS-CD8-GFP}{+}; \frac{landsite}{+}; \frac{RpS3*, act>RpS3>GAL4}{+}$
Figure 6	$\frac{hs-Flp, UAS-CD8-GFP}{+}; \frac{UAS-abruptRNAi(KK)}{+}; \frac{RpS3*, act>RpS3>GAL4}{+}$
Figure 7 & Figure 8	$\frac{Engal4, UAS-GFP}{UAS-abruptRNAi(KK)}$
Figure 8	$\frac{Engal4, GSTD1-GFP}{UAS-AbruptRNAi(KK)}; \frac{Xrp1-LacZ}{+}$
Figure 9	$\frac{hs-flp}{+}; \frac{Tub>STOP>Gal4, UAS-CD8-GFP}{abruptRNAi}; \frac{tub-GAL80TS}{+}$
Figure 9	$\frac{hs-flp}{+}; \frac{Tub>STOP>Gal4, UAS-CD8-GFP}{abruptRNAi}; \frac{tub-GAL80TS}{XRP1*(M273)}$
Figure 10	$\frac{hsflp}{+}; \frac{Frt40A, UbiGFP}{Frt40A, Abrupt(k02807)}$
Figure 11	$\frac{Frt40A, UbiGFP}{Frt40A, Abrupt(k02807)}; \frac{hh-Gal4, UAS-FLP}{+}$
Figure 12	$\frac{Tub-Gal4, UAS-CD8-GFP}{+}; \frac{tub-GAL80TS}{+};$
Figure 12	$\frac{Tub-Gal4, UAS-CD8-GFP}{UAS-AbruptRNAi(KK)}; \frac{tub-GAL80TS}{+};$
Figure 13	$\frac{GSTD1-GFP}{+}; \frac{UAS-AbruptRNAi(Trip)}{FRT82B, Rps3(Plac92), hh-GAL4}$
Figure 14	$\frac{En-Gal4, GSTD1-GFP}{+}; \frac{UAS-XRP1(Short)}{+}$
Figure 14 & Figure 15	$\frac{TubGal80ts}{+}; \frac{En-Gal4, GSTD1-GFP}{UAS-XRP1(Long)}$
Figure 16	$\frac{EnGal4, GSTD1-GFP}{+}; \frac{UAS-XRP1(HA)}{+}$
Figure 17	$\frac{GSTD1-GFP}{+}; \frac{FRT82B, Rps3(Plac92), hh-GAL4}{Irbp18-RNAi(HMS)}$
Figure 18	$\frac{GSTD1-GFP}{+}; \frac{FRT82B, Rps3(Plac92), hh-GAL4}{Perk-RNAi(35162)}$
Figure 18	$\frac{GSTD1-GFP}{Perk-RNAi(110278)}; \frac{FRT82B, Rps3(Plac92), hh-GAL4}{+}$
Figure 18 & Figure 19	$\frac{GSTD1-GFP}{Perk-RNAi(35162)}; \frac{FRT82B, Rps3(Plac92), hh-GAL4}{+}$

3.2 Fluorescencent staining

3.2.1 Antibody staining

All following steps were performed on rocking platform at room temperature (RT) unless otherwise indicated. For immunostaining, 3rd instar larvae were dissected in Phosphate buffered saline (PBS) solution. The posterior half of the larvae was removed, and the anterior portion inverted, revealing the wing discs. The dissected tissues were subsequently fixed with a 20-minute incubation in fixing solution: paraformaldehyde (PFA) diluted to 4 % in PBS. Fixed bodies were then permeabilized with 3 separate 10-minute washes using a PBST solution: triton TX-100 (Sigma, T9284) diluted to 0.25 % in PBS. After the permeabilization step, bodies were incubated in blocking solution: 4 % Fetal bovine serum (FBS) or Bovine serum albumin (BSA) (depending on antibody used) in PBS, for 30-minutes, followed by an overnight incubation on rocking platform in cold room (4 °C) with primary antibodies (Table 2) diluted in blocking solution. The next day, dissected bodies were washed 3 times for 10 minutes in PBST before incubating for an hour in secondary antibody solution in darkness (see Table 3). Finally, the wing discs and the mouth hooks of the stained bodies were separated in PBST and pipetted onto a standard glass microscope slide and excess liquid removed using a kimwipe. Dissected wing discs and mouth hooks were covered with a drop of VECTASHIELD® Antifade Mounting Medium H-1000 (Vector laboratories). Wing discs were then collected in the centre of the glass slide and moth hooks placed on the sides before placing a coverslip on top. The mouth hooks function as spacers to prevent the wing discs from being squashed under the coverslip. The coverslip was glued on using standard nail varnish and the slide stored at 4°C before imaging.

3.2.2 Translation assay (OPP)

For O-propargyl-puromycin (OPP) -based assays for translation a Click-iT® Plus OPP Protein Synthesis Assay Kit (C10458, Thermo Scientific). Larvae were dissected in PBS and dissected wing discs placed immediately in Schneider's medium (P04-90599, Pan Biotech). After dissection Click-iT® OPP Reagent was diluted in the Schneider's medium suspension to the concentration of 5 μM before incubating at 25 °C in a heat block for 15 minutes. Wing discs were subsequently rinsed twice in PBS and fixed in fixing solution (4 %PFA) for 20 minutes. Fixing solution was rinsed from wing discs with two PBS washes before permeabilization in PBST solution for 30 minutes, followed by a 30-minute incubation in 4 % FBS blocking solution. After a single rinse in PBS the wing discs were incubated for 25 minutes in Click-iT reaction mix for red fluorophore mixed according to manufacturer protocol. Click-iT reaction was then quenched via several short >5 PBS washes and 15-minute incubation in 1:5000 Hoechst in PBS solution followed by an additional 10-minute PBS wash. Stained wing discs were then mounted in PBST as usual (3.2.1).

3.2.3 List of Antibodies

The following antibodies were used for immunofluorescent staining of wing discs.

Table 2: List of primary antibodies

1°-Antibodies					
Name:	Target:	Species	Source:	Cat no:	Dilution used for staining:
Cleaved Drosophila Dcp-1 (Asp216) Antibody	Decapping protein 1 (Dcp1)	Rabbit	Cell Signalling Technologies	9578	1:500
Anti-ACTIVE® JNK pAb, Rabbit	Phosphorylated Janus terminal Kinase (JNK)	Rabbit	Promega	V793B	1:500
Anti-β-Galactosidase mAb	Anti-β-Galactosidase (GAL)	Mouse	Promega	Z3781	1:500
Phospho-eIF2α (Ser51) Antibody	Phosphorylated-(p-eIF2α)	Rabbit	Cell Signalling Technologies	D9G8XP	1:500
Anti-Ubiquitinylated proteins Antibody, clone FK2	Ubiquitinylated proteins	Mouse	Merck	4-263	1.500
HA Tag Monoclonal Antibody (5B1D10)	Haemagglutinin (HA)	Mouse	Invitrogen	32-6700	1:500

Ci Antibody	Cubitus interruptus (Ci)	Rabbit	Developmental Studies Hybridoma Bank (DSHB)	2A1	1:500
α-Abrupt	Abrupt (Ab)	Mouse	Developmental Studies Hybridoma Bank (DSHB)	Abrupt	1:20
anti-Grp78/BiP	Glucose Regulated Protein 78 (Grp78/Bip)	Rabbit	StressMarq	SPC180-C	1:5000

Table 3: List of secondary antibodies

2°-Antibodies				
Name:	Species:	Source:	Cat no:	Dilution used for staining
Donkey anti-Mouse IgG (H+L) Highly Cross-Adsorbed Secondary Antibody, Alexa Fluor Plus 488	Donkey	Thermo Scientific	A32766	1:500
Donkey anti-Rabbit IgG (H+L) Highly Cross-Adsorbed Secondary Antibody, Alexa Fluor Plus 488	Donkey	Thermo Scientific	A32790	1:500
Donkey anti-Mouse IgG (H+L) Highly Cross-Adsorbed Secondary Antibody, Alexa Fluor Plus 555	Donkey	Thermo Scientific	A32773	1:500
Donkey anti-Rabbit IgG (H+L) Highly Cross-Adsorbed Secondary Antibody, Alexa Fluor Plus 555	Donkey	Thermo Scientific	A32794	1:500
Donkey anti-Mouse IgG (H+L) Highly Cross-Adsorbed Secondary Antibody, Alexa Fluor Plus 647	Donkey	Thermo Scientific	A32787	1:500
Donkey anti-Rabbit IgG (H+L) Highly Cross-Adsorbed Secondary Antibody, Alexa Fluor Plus 647	Donkey	Thermo Scientific	A32795	1:500

3.3 Image acquisition and analysis

All prepared slide samples were imaged in a Leica SP8 inverted confocal microscope using a 40x HC PL Apo CS2 Oil objective (Leica, 11506329). Each wing disc was imaged as z-stacks with each section corresponding to 1 μM and captured images stored in .LIF format. Captured images were analysed and processed using the Fiji image processing software (Schindelin et al., 2012). Quantification of fluorescent signal and clone area was calculated using a Macro developed by PhD candidate Michael Baumgartner.

For each quantification, the wing pouch area was defined manually prior to processing by the Macro. For analysis of cross compartmental analysis, specific compartments of the wing discs (the Anterior and Posterior compartments) were assigned by hand. For mosaic wing discs, clonal areas were defined using a custom script built into the macro, where GFP-labelling served as the indicator of clones. All clone selections made by the macro were checked for accuracy before being used for quantification. For cell death quantifications of wing, cells positive for Dcp1 were counted in each specified region, where counts were normalized to the respective area measured in Fiji. To measure signal intensity, mean grey value of the SUM fluorescence of selected Z-slices was measured using Fiji for regions specified for each genotype within the pouch region of the wing disc.

3.4 DNA extraction and PCR

For the extraction of genomic DNA (gDNA) a DNeasy Blood and Tissue kit (69506, Qiagen) was used with buffers diluted according to manufacturer's instructions. Genomic DNA was extracted from adult fly tissue samples prepared by freezing 1-2 live adult flies in Eppendorf tubes at -20 °C for >20 minutes before macerating and suspending in PBS using a pestle.

3.5 RNA extraction

3.5.1 RNA extraction using separation columns

For high yield samples such as whole larvae, a RNeasy Mini Kit (74104, Qiagen) was used to extract RNA. Before RNA extraction all surfaces and lab tools involved were sprayed with a 70 % ethanol solution followed by a light spray of RNaseZap solution (Thermo Scientific) to prevent sample contamination. For each sample 1-4 whole 3rd instar larvae were crushed via pestle in lysis solution. The lysate could then be stored for several weeks at -20 or be used immediately for RNA extraction. Following the protocol supplied by manufacturer, RNA was extracted using separation columns and suspended in 30-50 µL of nuclease free water. The isolated RNA was then immediately reverse transcribed (see section 3.6) or stored at -20 °C for use within 24 hours.

3.5.2 RNA extraction using Trizol reagent

To extract RNA from low yield samples such as wing discs, Trizol reagent (15596018, Thermo Scientific) was used. Prior to Trizol based extraction all surfaces and lab tools involved were cleaned via 70 % ethanol or RNaseZap solution. Furthermore, as Trizol is a phenol-based reagent, all steps involving it were performed under a fume hood. In ice-cold PBS, 20 wing discs were dissected and placed PBS in 1.5 ml Eppendorf tube on ice before centrifuging at max speed (12.000g) for 1 minute. Supernatant was removed and wing discs resuspended in Trizol reagent to a final volume of 500µl and incubated at RT for 5 minutes to ensure complete lysis of tissue. The RNA lysate could then either be stored at -20 °C for long periods or used immediately. RNA was isolated from the Trizol reagent by adding 100µl of chloroform to the lysate and vortexing thoroughly for 15 seconds before incubating on ice for 2 minutes. The now partially separated lysate was centrifuged at max speed (12.000g) at 4 °C in order to separate the transparent RNA-containing aqueous layer from the other layers. The aqueous layer was then transferred via p200 pipette to a new Eppendorf tube and equal amount of isopropyl alcohol added and mixed thoroughly in a vortex before incubating overnight at 4 °C. Next the RNA was precipitated from the solution by centrifuging at max speed for 30 minutes at 4 °C, this separates RNA from the solution in form of a small clear pellet. Supernatant was removed and the pellet washed with ice cold 70 % ethanol solution and centrifuged again for 30 minutes at 4 °C. Supernatant aspirated again leaving behind a white pellet of pure RNA. Remaining ethanol was dried by leaving Eppendorf tube open upside down (to prevent contaminants entering the tube) for >1 hour at RT. The RNA pellet was then resuspended in nuclease free water (10-20µl) and either used immediately or stored in -20 °C freezer for use within 24 hours.

3.6 Reverse transcription

3.6.1 DNase treatment

To remove any potential trace amounts of DNA in extracted RNA samples (3.5.1 & 3.5.2) we treated every RNA sample with DNase prior to reverse transcription (3.6.2). DNase treatment was conducted according to instructions and protocol provided by Remi Logeay, a postdoctoral fellow in our lab. In a 0.2 ml PCR-strip tube, 5 µl of DNAse buffer solution (Thermo Scientific, 8170G), 2 µL of DNase enzyme solution (Thermo Scientific, AM2222), and 1 µl of RNAse OUT™ Recombinant Ribonuclease Inhibitor (Thermo Scientific, 10777019) were mixed with RNA sample solution (up to 10 µg RNA) and topped up to 50 µl with nuclease free water. The mixture was then incubated at 37 °C for 30 minutes followed by a 10 minute 75 °C DNase heat inactivation incubation in a Veriti™ 96-Well Thermal Cycler (Applied Biosystems, 4375786).

3.6.2 Reverse transcription

Following DNase treatment, the nucleotide concentration of RNA samples was measured via Nanodrop 1000 (Thermo Scientific) before proceeding to reverse transcription steps. As varying RNA concentration can affect the efficiency of reverse transcriptase enzymes, equal amounts of RNA were used for samples intended for transcriptional comparison. Reverse transcription was performed following protocol and using reagents provided by the Invitrogen SuperScript™ III Reverse Transcriptase kit (18080-093, Invitrogen). Prepared cDNA was stored at -20 °C for later use.

3.7 Quantitative Real-Time PCR (qPCR)

For the quantification of expression of specific genes, quantitative PCR (qPCR) was used. All qPCR reactions were performed using reagents and following protocol included in the QuantiNova SYBR Green PCR Kit (208052, QuantiNova). Prior to use, ROX dye was added to the SYBR Green I reaction mixture according to manufacturer's instructions. Primers were acquired from various sources (Table 4) and diluted to 10 μM in nuclease free water prior to use. The efficiency of each primer combination was calculated using the Ct slope values of cDNA serial dilutions (Pfaffl, 2001). Reactions were set up in MicroAmp™ Optical 96-Well Reaction Plates (N8010560, Thermo Fisher) and run using a StepOne™ Real-Time PCR System (4376357, Applied Biosystems) using temperature cycle conditions provided by the SYBR Green PCR kit. Results were digitally processed using integrated StepOne™ Software v2.3 (Applied biosystems). Quantification and analysis of qPCR results are discussed in a separate chapter (3.8.2).

Table 4: Oligonucleotides used in this project.

Primer target:	Fwd/Rev	Sequence	Source
1731-repetitive-element reverse transcriptase (*1731*)	Fwd	TATGGGCTGAGGCGATAAAC	Sigma Aldrich
	Rev	CAAGTGGCTCACTGCTGGTA	
abrupt	Fwd	CTCCAGGGCATTCCAGGACTTC	Sigma Aldrich
	Rev	ATCTGTGGCTCGGACTCGCAT	
Actin 5C *(act5c)*	Fwd	AAGTTGCTGCTCTGGTTGTCG	Sigma Aldrich
	Rev	GCCACACGCAGCTCATTGTAG	
Argonaute 2 (*ago2*)	Fwd	CAAGAAAGGAGGACAGGATAGC	Sigma Aldrich
	Rev	TTGTTGCTGATGCGGTTG	
copia	Fwd	CTTTTAGCCGAGCAAGATGTG	Sigma Aldrich
	Rev	CATAAACGGCGTCCAAATTCTC	
septin interacting protein 3 (*sip3*)	Fwd	CTTCAATCCGCGCTTTGTGGCC	Sigma Aldrich
	Rev	TGCCTAGCACTGTGAGCAGACT	
tonalli	Fwd	CAGTGGCCAAAGTGCTGGAATG	Sigma Aldrich
	Rev	TGCCAGGAACTGGACTGTGCTG	
Xrp1 (RA, RC, RE, RG-)	Fwd	TCATCGCGGAACAATAACAGTG	(Lee et al., 2018)
	Rev	GCAATAGGTTGGGTGGTTCC	

3.8 Statistics

3.8.1 Confocal

To validate statistical significance of processed image results (see section 3.321) an application, also developed by PhD candidate Michael Baumgartner, based on the R-programming language, was used. This app recognises processed image data files in .csv format outputted by the Macro and automatically sets them up for the user for further statistical analysis. Using this tool, statistical significance of image data was measured in the form of P-values using an unpaired two-tail t-test, Wilcoxon rank sum test or Wilcoxon signed rank test based on the dataset (see figure legends for which test was used). Statistical significance is indicated with an asterisk (*) which was defined with the threshold p-value of $p \leq 0.05$, where p-values above this threshold are considered non-significant. Lower p-values contribute to higher degrees of significance indicated by increasing number of asterisks: $p \leq 0.05$(*), $p \leq 0.01$ (**), $p \leq 0.001$ (***).

3.8.2 Quantitative Polymerase chain reaction (qPCR)

To ensure statistical significance at least 2 biological replicates, unless otherwise indicated, were used for transcriptional analysis using qPCR. Furthermore, for each qPCR run, triplicate technical repeats were measured to prevent deviation due to pipetting or other environmental factors. Prior to export, amplification plots and melting curves were observed for signs of contamination or primer dimers, which if found all data from affected wells were omitted from calculations. All Ct (Cycle threshold) values were exported from the integrated StepOne™ Software in .Xls format and relative expression ratio calculations made using Microsoft Excel. The relative expression ratio of target genes was calculated using the ΔΔCt method which assumes that the amplification of all used primers doubles the target sequence per cycle. Only primers with efficiency above 90 % were used in this project to minimise the effect of varying primer efficiency. Standard deviation of each triplicate sample Ct values were measured, and if the standard deviation of a triplicate sample exceeded 0.5, they were not considered reliable. If the deviation was caused by a single repeat it could sometimes be omitted from calculations leaving two repeats behind for further processing. To validate the significance of change in relative expression of target genes a standard t-test was performed using a standard unpaired two-tailed t-test (student's test) using Excel by Microsoft, where the degree of significance was indicated by number of asterisks as described previously (3.8.1).

4 Investigating the function of Abrupt in cell competition

4.1 Rationale

Preliminary data from the RNAi screen had identified several candidate genes with a potential role in cell competition. Among those candidates was Abrupt, a BTB-zinc finger transcription factor involved with various processes including regulation of epithelial cell growth (Turkel et al., 2013). When the *abrupt-RNAi (KK)* line (VDRC ID: 104582) was expressed in $RpS3^{+/-}$ clones using the MIWO tool it resulted in increased border cell death and reduced clone size compared to control $RpS3^{+/-}$ clones.

Due to the pronounced competitive effects produced by the expression of the *abrupt-RNAi (KK)* line, we investigated *abrupt* further in order to understand what drives this enhanced competitive phenotype. To achieve this, we used various competitive assays, as well as transcriptional analysis, measuring how *abrupt* affects other competitive factors. In addition to *abrupt* we sought to investigate the competitive properties of other genes identified in the screen, potentially linking them to pathways known to be involved in the process of cell competition. By seeking out new regulators of cell competition we hoped to gain further insight into what drives and maintains cell competition, specifically what drives cells to become losers, hopefully yielding a more comprehensive model of the process.

4.2 Results

4.2.1 The *abrupt*-RNAi (KK) line enhances cell competition

At the start of the project we determined whether the results of the RNAi screening were reproducible by expressing the *abrupt-RNAi (KK)* line in *RpS3* clones in a WT background using the Miwo tool (see methods 3.1.2). As a control for the $RpS3^{+/-}$, *abrupt-RNAi (KK)* clones, we generated $RpS3^{+/-}$ clones with an empty *attP*-site insertion. Consistent with the results of the RNAi screen the $RpS3^{+/-}$, *abrupt-RNAi (KK)* clones showed a significantly higher border cell death as well as consistently smaller clones compared to control $RpS3^{+/-}$ clones (Figure 6). This suggested that expressing the *abrupt-RNAi (KK)* line in loser $RpS3^{+/-}$ clones enhanced their loser status increasing the rate of their elimination by the surrounding WT cells.

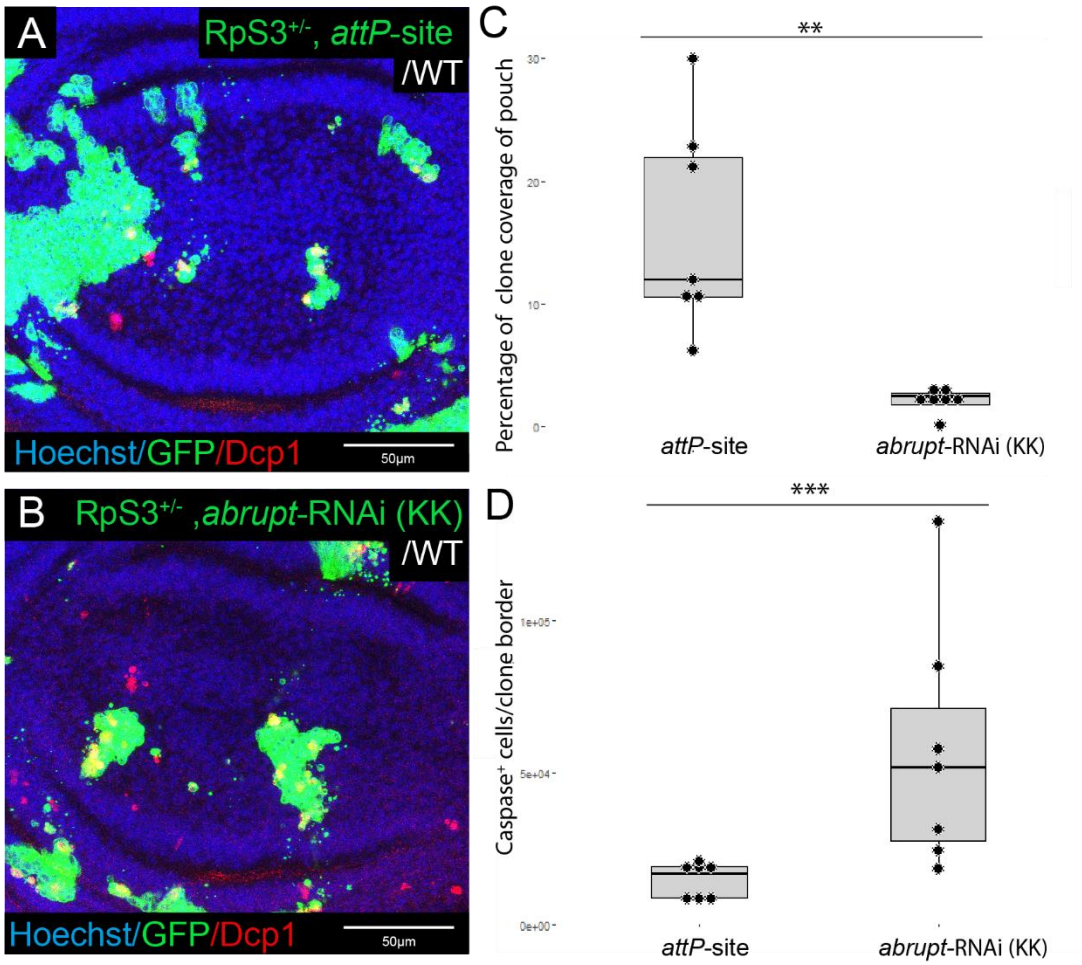

Figure 6: *abrupt*-RNAi (KK) line enhances competition.

(A) : $RpS3^{+/-}$ clones (Green) with a control att-site (Landing site) generated in a WT *Drosophila* wing discs with hoechst nuclear labelling. (B) : $RpS3^{+/-}$ clones (Green) discs expressing *the abrupt*-RNAi (KK) line generated in a WT *Drosophila* wing pouch with hoechst nuclear labelling. (C) Percentage of wing pouch area (defined selection of Z-levels within the pouch region of the wing disc) occupied by clones (7 technical repeats, unpaired two-tail t-test: $p = 0.0023$). (D) Percent caspase coverage on clone borders (7 technical repeats, unpaired two-tail t-test: $p = 0.00058$).

Given that the *abrupt-RNAi (KK)* clones were eliminated at an enhanced rate, we speculated whether the oxidative stress pathway, which has been shown to be activated in loser cells, might be affected by the *abrupt*-RNAi (KK) line. To measure Nrf2 activation, we expressed the *abrupt*-RNAi (KK) line in the posterior compartment with the *engrailed*-GAL4 (*en*-GAL4) driver in flies harbouring the transgenic *GstD1-GFP* reporter, which consists of Glutathione S-Transferase (*GstD1*) promoter sequence upstream of the *GFP*. As *GstD1* is a transcriptional target of Nrf2 it serves as an indicator for relative Nrf2 activity. Image analysis of these discs showed strong *GstD1*-GFP signal in the *abrupt*-RNAi (KK) expressing posterior compartment compared to the anterior control cells. (Figure 7). Quantification showed that the *abrupt*-RNAi (KK) line significantly upregulates Nrf2 activation to comparable or potentially higher levels than those measured in other prospective loser cells such as *Minutes*. Given the clear upregulation of Nrf2 in *abrupt-RNAi (KK)* expressing wing discs, we sought to assess whether other defects associated with the *Minute* phenotype were also affected. We began by measuring the rate of translation in *abrupt-RNAi (KK)* expressing wing discs, as impaired translation is among the defining features among *Minute* heterozygous flies. To measure translational rates, we performed an OPP assay which stains for newly synthesised polypeptides in a cell. Using this method, we found a substantial decrease in translation in the *abrupt*-RNAi expressing posterior compartment of *en*-GAL4>*abrupt-RNAi (KK)* wing discs (Figure 7). Preliminary results from our lab have found JNK to be upregulated in transcriptionally impaired cells (Dinan, 2018), which prompted us to pursue the relation between *abrupt*-RNAi (KK) line and JNK activity. Assessment of JNK pathway activity via anti phosphorylated JNK antibody (p-JNK) immunostaining in *abrupt*-RNAi (KK) line expressing cells revealed a considerable increase in JNK activation (Figure 7).

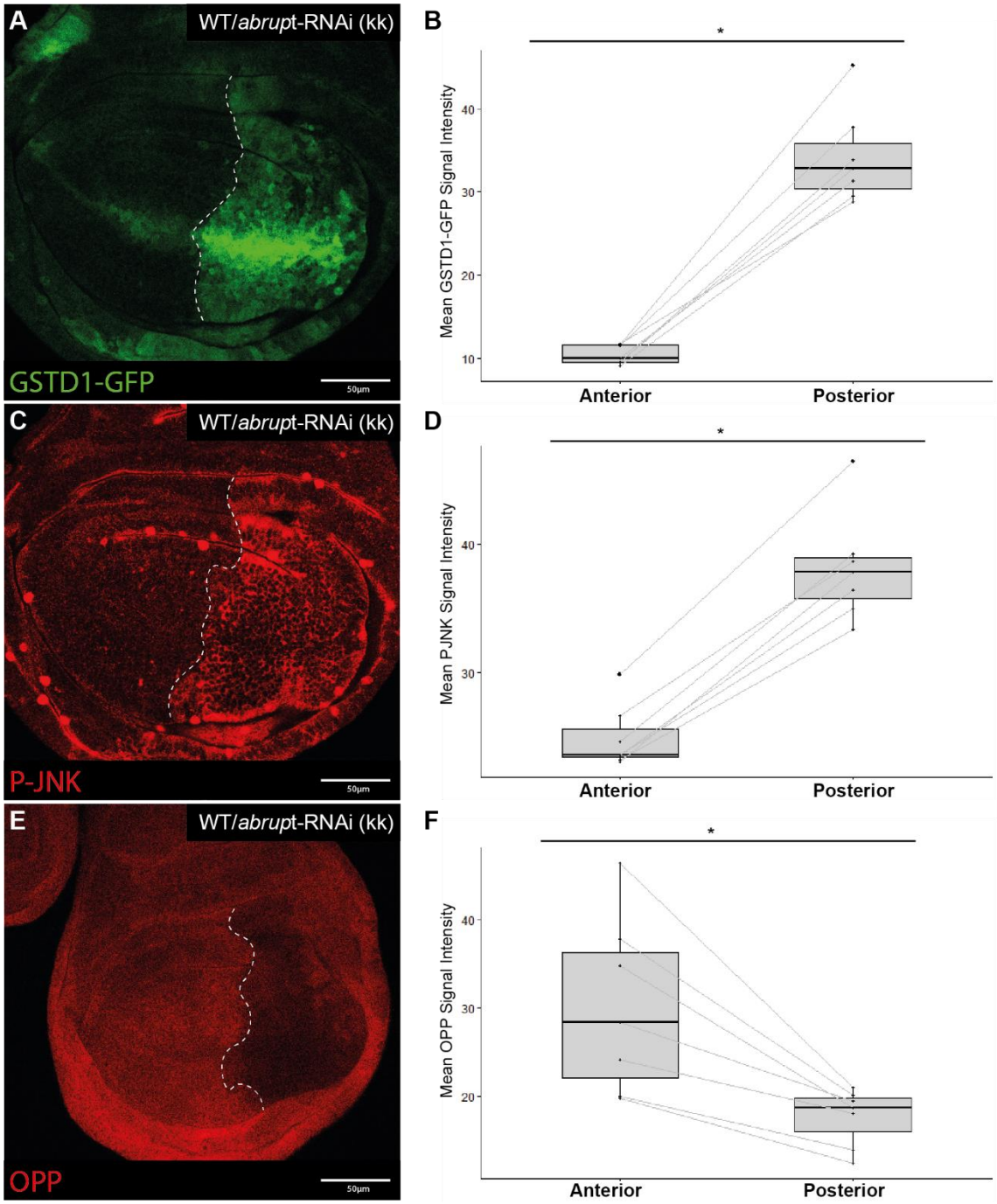

Figure 7:The effect of *abrupt*-RNAi (KK) line effect on oxidative stress pathway and translation.

The *abrupt*-RNAi (KK) line was specifically expressed in the posterior compartment (Right) using the *en*-GAL4 driver A-B) Activation of Nrf2 measured in wing discs via GSTD1-GFP marker (Green) (6 technical repeats, Wilcoxon Signed Rank test p = 0.02). C-D) Phosphorylation of JNK measured via α-p-JNK specific antibody (Red) (6 technical repeats, Wilcoxon signed rank test p = 0.02). E-F) Translational efficiency measured via OPP assay (Red) (Methods: 3.2.2) (5 technical repeats, Wilcoxon signed rank test p = 0.02).

Enhanced levels of proteotoxic stress is another feature commonly shared by prospective loser phenotypes (Dinan, 2018). Given that the *abrupt*-RNAi affected other loser markers in a manner characteristic of losers, we anticipated elevated levels of proteotoxic stress levels to be present in *abrupt*-RNAi expressing wing discs. As a readout of proteotoxic stress we measured the activation of the proteotoxic stress response factor eIF2α, which shuts down global translation in response to enhanced proteotoxic stress. We observed activation of eIF2α by measuring its phosphorylation via antibody staining. With this we could observe a significant increase in phosphorylated-eIF2α (p-eIF2α), it's active form, in the posterior *abrupt*-RNAi expressing compartment (Figure 8), which, along with the elevated levels of JNK and Nrf2 activation and impaired translation, suggested that the *abrupt*-RNAi (KK) line is causing a particularly strong loser phenotype. Given how many pathways associated with *Minute* mutations were influenced by the *abrupt*-RNAi (KK) line we hypothesised that Abrupt could potentially be involved in the regulation of an upstream factor in the signalling network that responds to *Minute* mutations. The transcription factor Xrp1 has been proposed to be an upstream regulator of many pathways associated with competition including JNK and Nrf2 and furthermore is highly upregulated in prospective losers, including *Minute* cells (Baillon et al., 2018, Blanco et al., 2020, Kucinski et al., 2017). We therefore sought to measure Xrp1 expression in *abrupt*-RNAi (KK) expressing cells to determine if the alterations in stress pathways are due to downstream effects of Xrp1.

We expressed the *abrupt*-RNAi (KK) line in the posterior compartment of wing discs carrying a transcriptional reporter for Xrp1, which is a LacZ gene containing P-element inserted in the Xrp1 locus (Xrp1-LacZ). By staining the wing discs for β-Galactosidase, the encoded product of LacZ, we could measure the relative expression of Xrp1. The β-Galactosidase staining of *xrp1-lacZ* wing discs revealed an upregulation of Xrp1 expression in *abrupt*-RNAi (KK) expressing cells indicating the activation of the proteotoxic and oxidative stress pathways as well as impaired translation could all therefore be due to a downstream effect of the upregulation of Xrp1. This led us to pursue the relationship between Xrp1 and the *abrupt*-RNAi (KK) line further to identify whether Xrp1 is the driver of the loser status in *abrupt*-RNAi (KK) line expressing cells.

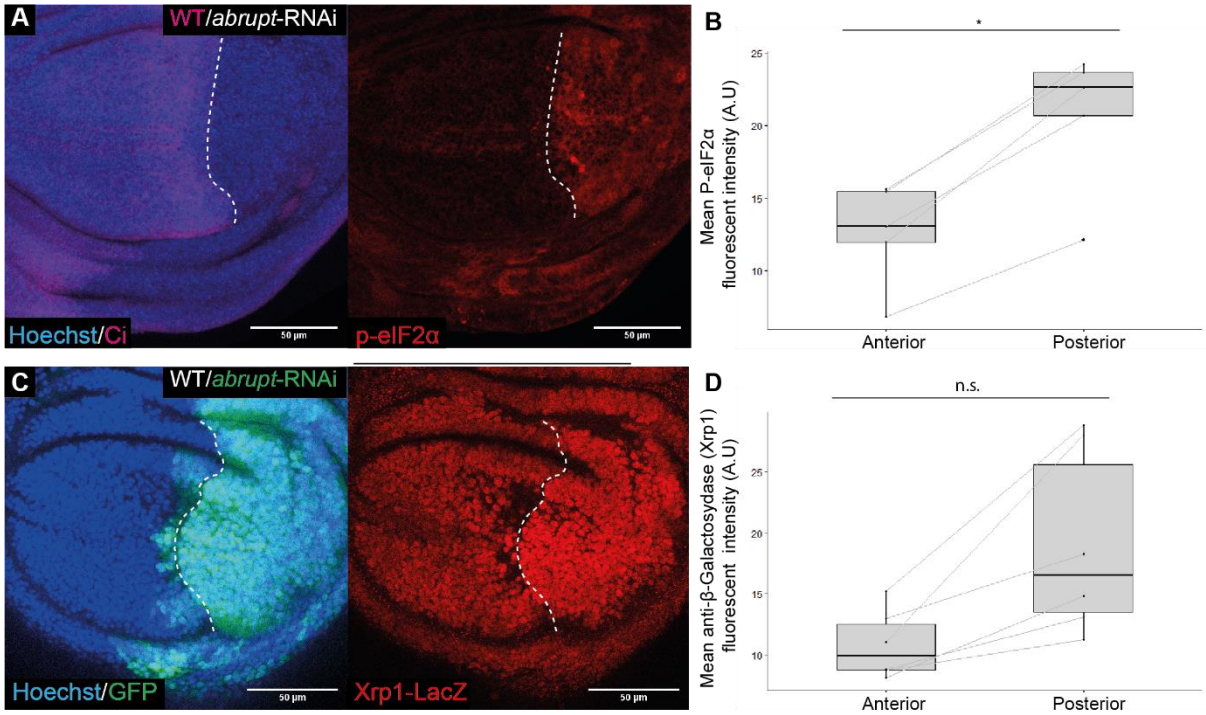

Figure 8: p-eIF2α and Xrp1 are elevated in *abrupt*-RNAi (KK) cells.

(A) A WT wing disc with posterior compartment specific expression of *abrupt*-RNAi (KK) and GFP (not shown) under the *engrailed*-GAL4 driver (*en*-GAL4). The anterior compartment marked with anti-Ci antibody (Magenta), cell nuclei labelled with Hoechst. The difference in eIF2α activity between compartments is measured with anti-p-eIF2α antibody (Red). (B) Mean p-eIF2α signal intensity between anterior and posterior compartment of wing disc shown in A (4 technical repeats, Wilcoxon signed Rank test p = 0.02). (C) Similar wing disc as in A, showing GFP and Hoechst nuclear labelling. Expression of Xrp1-LacZ is measured via anti-β-galactosydase antibody (Red). (D) Mean anti-β-galactosidase fluorescent intensity in anterior and posterior compartment of wing discs represented in C, (5 technical repeats, Wilcoxon signed rank test p = 0.06).

4.2.2 Xrp1 inhibition rescues *abrupt*-RNAi loser phenotype

To test whether *abrupt*-RNAi enhances the loser status of *Minute* cells through Xrp1 we generated *abrupt-RNAi (KK)* clones in a Xrp1 loss of function mutant ($Xrp1^{M2\text{-}73/+}$) background and WT background as a control. As the *abrupt*-RNAi (KK) line causes cells to be eliminated rapidly, large clones (covering most of the wing disc) were generated by inducing clones on day 2 (see Figure 4). The $Xrp1^{M2\text{-}73}$ mutation is a G-T truncated mutation which should lack the AT hook and bZip DNA-binding domains. Induced *abrupt*-RNAi (KK) clones grew significantly larger in an $Xrp1^{M2\text{-}73}$ heterozygous background in comparison to WT indicating an almost complete rescue of competitive elimination (Figure 9). Additionally, anti-caspase immunostainings showed that cell death was considerably lower in the Xrp1 mutant background, reaching comparable levels to healthy WT wing discs, while in the WT background the *abrupt*-RNAi clones had high levels of caspase activity as could be observed in previous experiments (Figure 9). These results strongly pointed towards Xrp1 functioning as the primary driver of competition in *abrupt*-RNAi clones, but how the *abrupt*-RNAi mediated the upregulation of Xrp1 remains unclear.

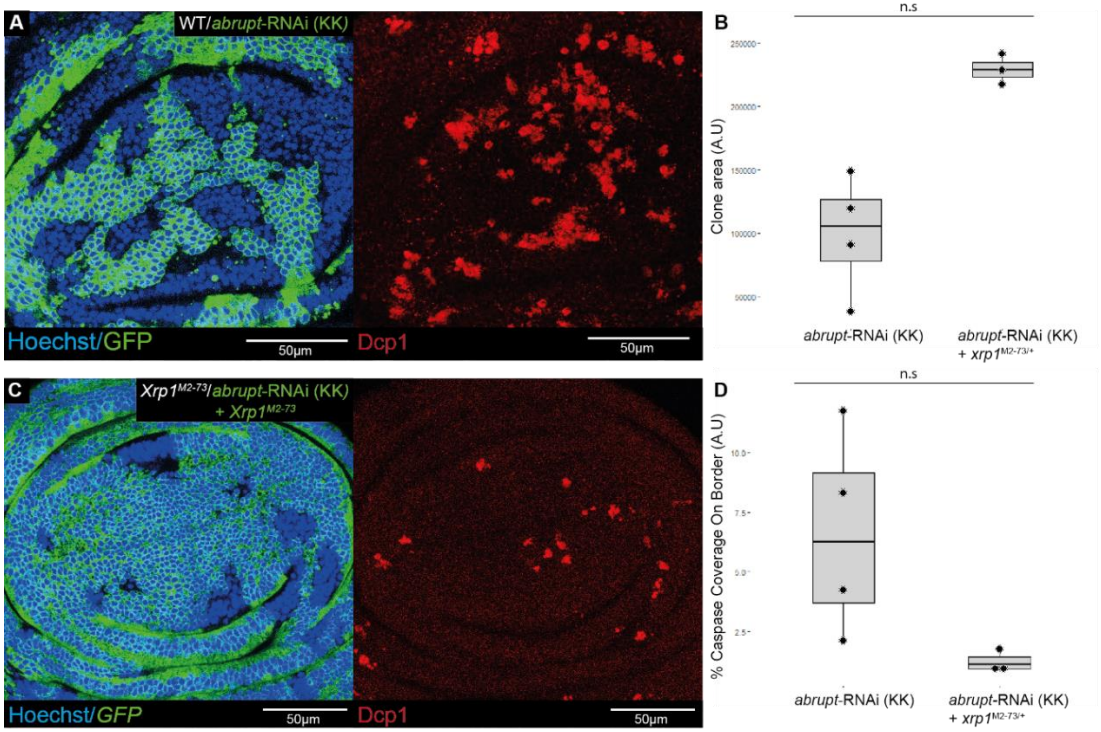

Figure 9: Inhibition of Xrp1 in *abrupt*-RNAi clones in a WT background rescues them from elimination.

(A) **:** GFP labelled clones (Green) expressing *abrupt*-RNAi (KK) line, generated in a WT wing disc (clones induced on day 2 to produce larger initial clones (see Figure 4)) with Hoechst nuclear labelling (B) Clone area of *abrupt*-RNAi (KK) clones in WT disc and *abrupt*-RNAi (KK) clones in $Xrp1^{M2\text{-}73/+}$ discs (4 technical repeats, unpaired t-test p = 0.057). (C) *abrupt*-RNAi (KK) line expressing clones (Green) genereated in an *Xrp1* heterozygous *Drosophila* wing disc with Hoechst nuclear labelling. (D) Percent caspase coverage of *abrupt*-RNAi (KK) clone borders in WT wing disc and *abrupt*-RNAi (KK) clone borders in $Xrp1^{M2\text{-}73/+}$ discs (4 technical repeats, unpaired t-test p = 0.011)

4.2.3 Identifying off targets of *abrupt*-RNAi

To confirm the function of Abrupt in cell-competition we tested Abrupt loss of function mutations to see whether mutant clones would be outcompeted by wildtype cells. We started by testing $abrupt^{P}$, an Abrupt mutant line containing a P-element insertion which was found to produce the Abrupt-vein phenotype in adult flies which is indicative of loss of function (Bejarano et al., 2012). Clones homozygous for the $abrupt^{P}$ mutation were generated (see methods 3.1.3) stained and imaged for border cell death and activation of stress pathways. No noticeable border cell death could be observed by Dcp1 staining indicating that the $abrupt^{P}$ mutation is not sufficient to induce competition (Figure 10). Stress pathways also appear to be unaffected by the $abrupt^{P}$ mutation as neither p-JNK or p-eIF2α antibody stainings showed any significant change in expression (Figure 10). As little was known of the effect of the $abrupt^{P}$ insertion we reasoned that the lack of effect was because the mutation did not cause a complete loss of function.

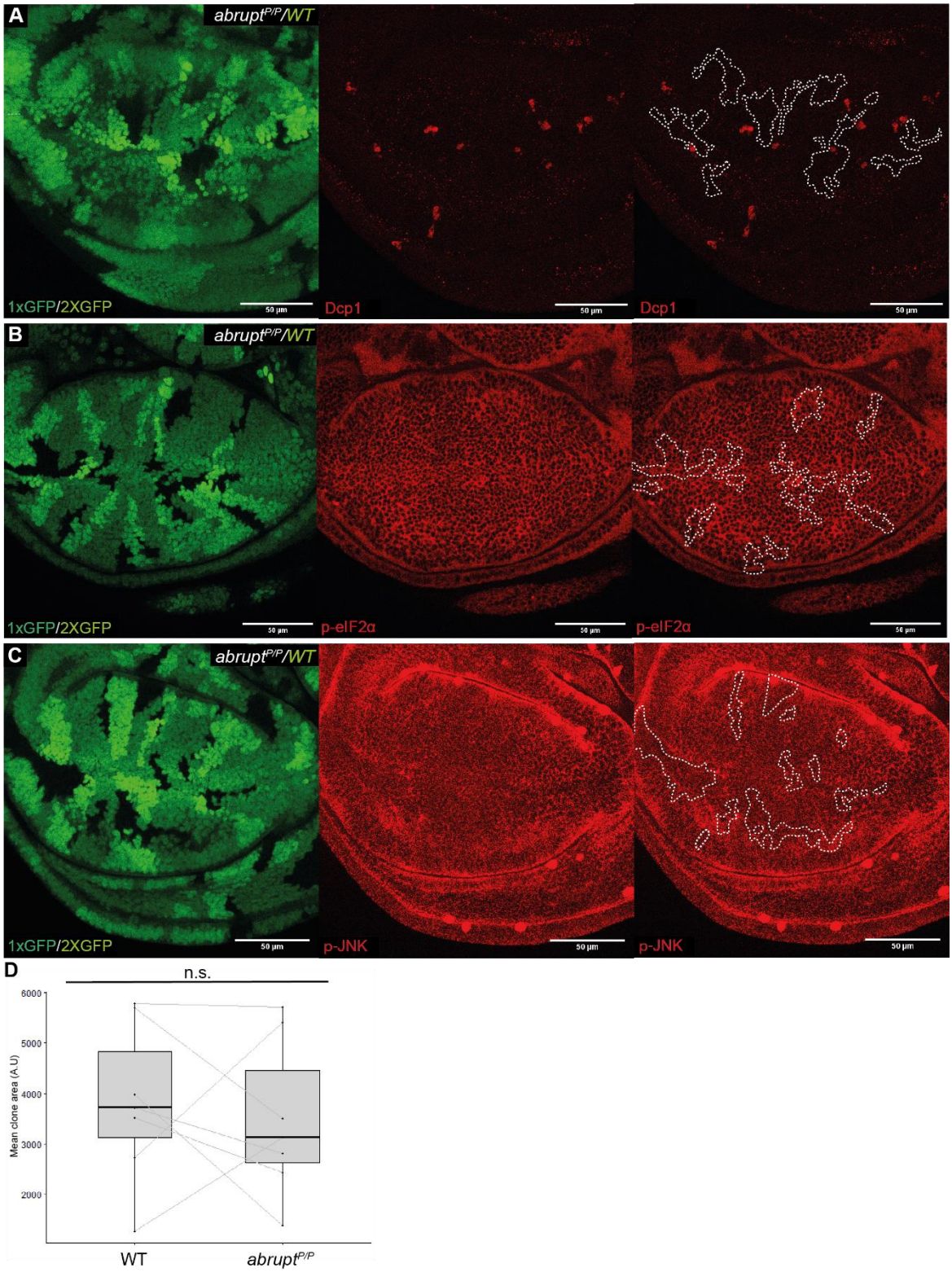

Figure 10: Abrupt mutant (Abrupt^{P}) clones do not affect cell death or stress pathway activation.

Abrupt mutant clones were generated via mitotic recombination (see methods 3.1.3). Clones homozygous for a P-element insertion mutation of *abrupt* (*abrupt*$^{P/P}$) are GFP negative (Black). (A) Mitotic *abrupt*$^{P/P}$ clones stained for death caspase 1 (Dcp1), *abrupt*^{P} clones outlined (B) Mitotic *abrupt*$^{P/P}$ clones stained for phosphorylated eIF2α (p-eIF2α), *abrup*$^{P/P}$ clones outlined. (C) Mitotic *abrupt*$^{P/P}$ clones stained for phosphorylated-JNK (p-JNK), *abrupt*$^{P/P}$ clones outlined. (D) Mean clone area of *abrupt*$^{P/P}$ clones and WT clones in wing discs shown in C (technical repeats, unpaired two-tail t-test: p = 0.69).

To test whether activation of stress pathways could be reproduced with a separate *abrupt* genotype, we used the loss-of-function *abrupt*^{1D} mutation, which has been previously shown to cause reduced levels of expression, and is reported to be a null allele (Turkel et al., 2013). The *abrupt*^{1D} mutation gives the Abrupt-vein phenotype when crossed to the homozygous viable *abrupt*^{1} allele (observation by Paul Langton), indicating that *abrupt* is indeed being downregulated. Clones homozygous for *abrupt*^{1D} were generated in the posterior compartment by mitotic recombination using the *hedgehog-flp* (*hh-flp*) construct (Figure 11). Caspase staining of *abrupt*^{1D} clones showed no significant border cell death, which enhanced our suspicion that the competitive effects seen in *abrupt*-RNAi (KK) expressing wing discs were due to an off-target RNAi effect. Furthermore, *hh-flp* induces clones early in development so the presence of large *abrupt* mutant clones at the end of larval development when the discs were dissected suggested that the mutant clones were not being out-competed by neighbouring wildtype cells. Using the same *hh-flp* construct we generated *abrupt*^{P} clones, which had a similar lack of effect on border cell death as *abrupt*^{1D} clones (Figure 11).

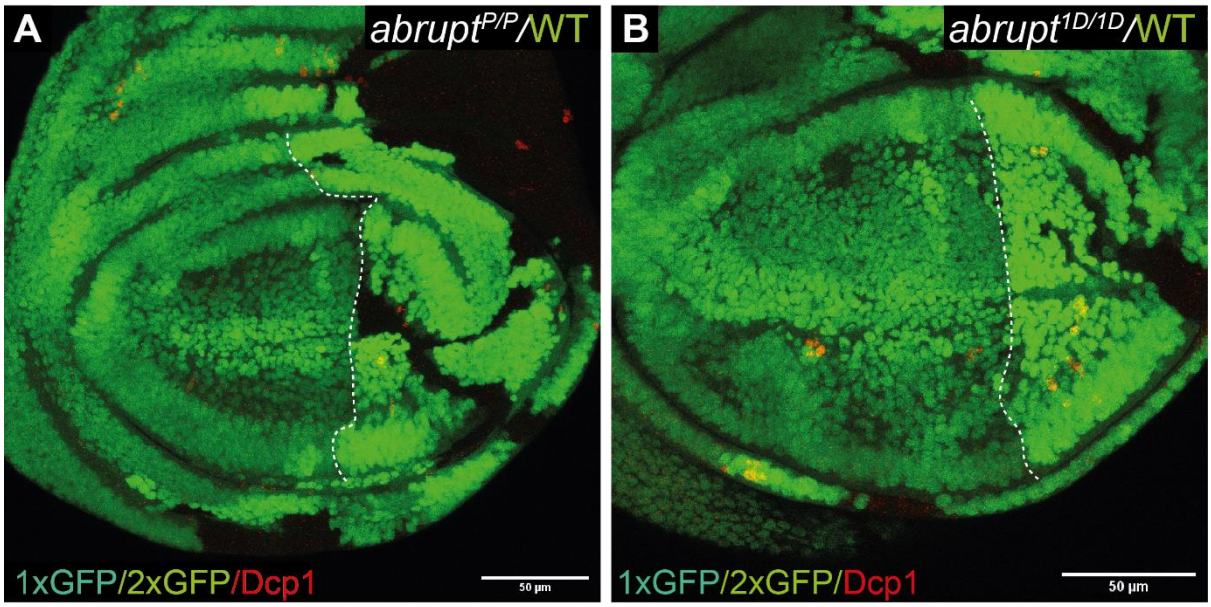

Figure 11: Abrupt mutant clones do not display enhanced border cell elimination.

Mitotic clones generated in the posterior compartment using *hedgehog*-Flippase construct (*hh-flp*). (A) A disc with mitotic clones in the posterior compartment, which are homozygous for *abrupt* P-element insertion mutation (*abrupt*^{P}) (GFP negative), or WT (2xGFP) and stained for Death caspase 1 (Dcp1) (Red). The anterior compartment is heterozygous for *abrupt*^{P} (1xGFP). (B) A similar wing disc as shown in A, but *abrupt*^{1D} clones (GFP negative) and stained for Dcp1.

To determine whether the *abrupt*-RNAi (KK) line targets *abrupt*, we measured relative expression of *abrupt* in wing discs ubiquitously expressing *abrupt*-RNAi (KK) under the *tubulin*-GAL4 driver with the temperature sensitive GAL80 inhibitor ($GAL80^{TS}$). in the background to avoid lethality caused by ubiquitous *abrupt*-RNAi (KK) expression. Control discs were the same genetic background but lacking the *abrupt*-RNAi (KK) construct. Both control and *abrupt*-RNAi (KK) crosses were incubated at 28 °C before dissection and RNA extraction. Relative expression of target genes was measured using qPCR (see methods 3.7) of cDNA transcribed from RNA extracted from wing discs. Quantification of the transcript of *abrupt* in *abrupt*-RNAi (KK) line expressing wing discs showed that abrupt was not being downregulated in *abrupt*-RNAi (KK) wing discs but was instead slightly upregulated (Figure 12). This upregulation of *abrupt* was not entirely unexpected because if the *abrupt*-RNAi (KK) line is mediating the loser status without targeting *abrupt* itself, the upregulation of *abrupt* may be a compensatory response to acquiring the loser status, as, in *Minute* discs *abrupt* has been shown by RNA sequencing to be upregulated (Kucinski et al., 2017).

Alongside *abrupt*, we also measured relative *xrp1* expression which, consistent with measurements made with the Xrp1-LacZ reporter (Figure 8), was highly upregulated in *abrupt*-RNAi (KK) wing discs. Since the *abrupt*-RNAi (KK) line was found not to target *abrupt*, this presented a unique challenge for us as its expression displays all indicators of an enhanced loser phenotype. We therefore sought to identify potential off targets to determine mechanisms by which the *abrupt*-RNAi (KK) line drives cells to become losers. By checking the sequence homology of the hairpin within the *abrupt*-RNAi (KK) construct to the *Drosophila* genome, Paul Langton identified two likely off target genes: *sip3* and *tonalli*. Since *sip3* functions in the ER-stress pathway it seemed like a promising candidate as its inhibition could enhance ER-stress. Less is known about *tonalli* aside for its function in transcriptional activation. However, neither *sip3* nor *tonalli* were found to be differentially expressed in the *abrupt*-RNAi wing discs in comparison to the control samples. Using a separate RNAi off-target identification tool Paul found *argonaute 2* (*ago2*) to be a likely off target. Like the other off-target candidates however, *ago2* was not significantly differentially expressed. In addition to measuring potential off targets of the *abrupt*-RNAi line, we also measured the levels of expression of two transposable elements; *copia* and *1731*, both of which have been found to be highly upregulated in *Minute* cells. The levels of expression of the transposons dwarfed the already high expression of *xrp1* in the *abrupt*-RNAi samples (Figure 12). These high levels of expression of transposons are not uncommon in loser genotypes and other members of the lab have observed similarly elevated levels of expression in other prospective loser mutants.

Since an off target could not be identified via qPCR, we had difficulty producing another method to test the target of the *abrupt*-RNAi (KK) line. Although a more in depth transcriptional approach such as the RNA sequencing of *abrupt*-RNAi (KK) samples would potentially provide some insight into the transcriptional environment of the cells, it would not be sufficient to provide enough evidence for the identification of an off target.

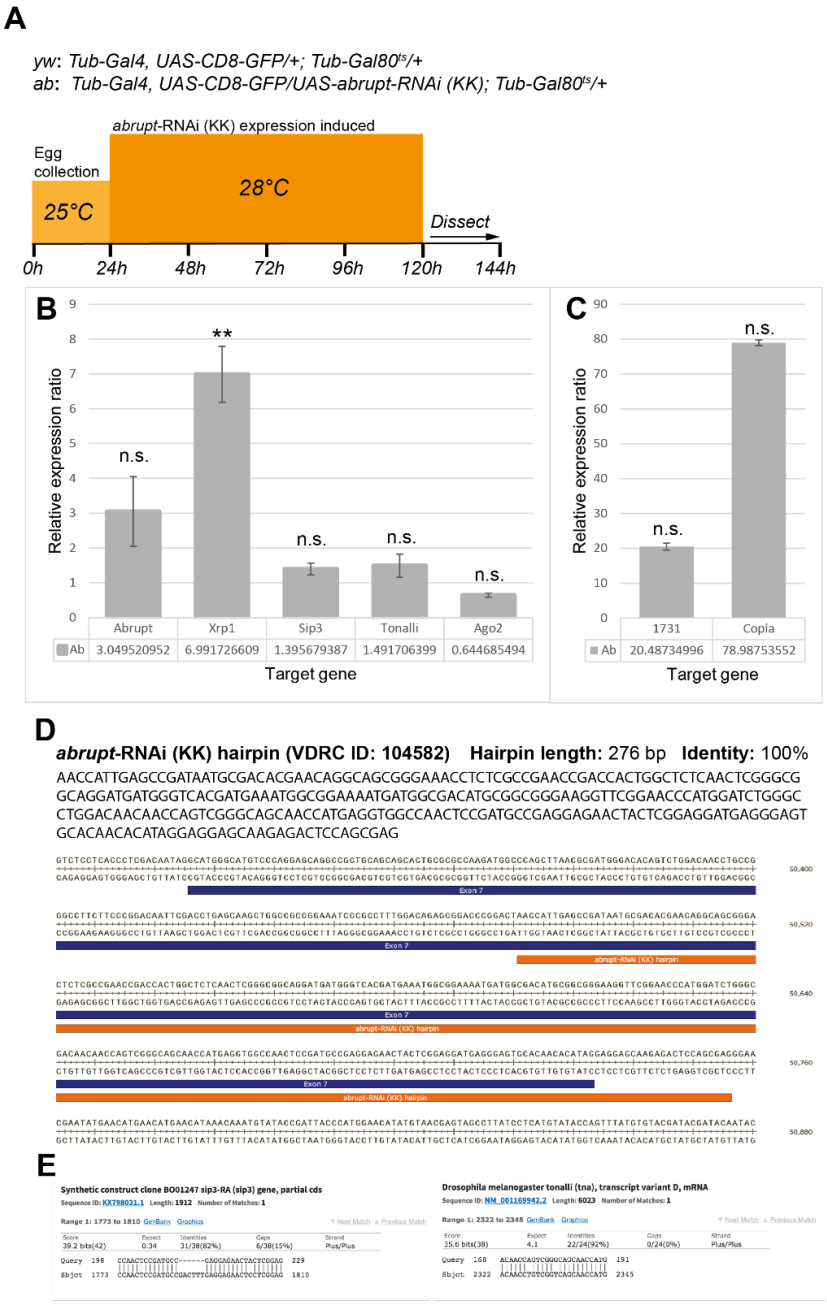

Figure 12: The *abrupt*-RNAi (KK) line does not target *abrupt* but causes a stong upregulation of Xrp1.

(A) Schematic representation of the genotypes and conditions selected for the preparation of samples for qPCR. Yellow white (Yw) control sample and *abrupt*-RNAi (KK) line (Ab) sample. (B) Relative expression ratio of genes in *abrupt*-RNAi (KK) expressing discs compared to control discs, calculated via the ΔΔCt method. Statistical significance calculated with unpaired two-tailed t-test: *abrupt* (3 Biological repeats, run in triplicates repeats each, p = 0.053), *xrp1* (3 Biological repeats, run in triplicates, p = 0.0043), *septin interacting protein 3* (*sip3*) (2 Biological repeats, run in triplicates, p = 0.48), *tonalli* (*tna*) (2 Biological repeats, run in triplicates, p = 0.73), Ago2 (2 Biological repeats, 3 Technical repeats each, p = 0.92). (C) Relative expression of transposable elements *1731* and *copia* in *abrupt*-RNAi (KK) discs compared to control discs, no statistical test was performed for 1731 and Copia expresion as data is derived from a single biological replicate (run in triplicates). (D) Sequence of the *abrupt*-RNAi (KK) hairpin with hairpin length and sequence identity to *abrupt trancript variants F, D, A and B* (according to NCBI BLAST tool). Below is shown sequence alignment of abrupt-RNAi (KK) hairpin (orange) to exon 7 (blue) in *abrupt* coding sequence. (D) Sequence homology analysis of a portion of the abrupt-RNAi (KK) hairpin to *sip3* and *tonally* (*tna*) preformed by Paul Langton using NCBI blast.

As the competitive effects of the *abrupt*-RNAi (KK) line were found to be likely due to an off-target effect, and it was still unclear how to identify its true target we opted to investigate another *abrupt*-RNAi line whose expression was found to cause the Abrupt-vein phenotype when expressed in wing discs. This *abrupt*-RNAi (Trip) line had been previously measured for Nrf2 activation, but due to the low signal produced compared to the results of the KK line, we thought at the time the RNAi-line might be inefficient. We tested the *abrupt*-RNAi (trip) line again, this time by expressing it in the posterior compartment of $RpS3^{+/-}$ wing discs with the *GstD1*-GFP reporter in the background to assay Nrf2 activation. Although not enough wing discs were imaged to acquire statistical significance, they did display a noticeable trend towards increased Nrf2 activation (Figure 13) suggesting Abrupt may play a role in the regulation of the oxidative response in *Minute* cells. Based on the p-eIF2α antibody staining (Figure 13) The *abrupt*-RNAi (Trip line) does not appear to significantly affect activation of eIF2α. This suggests that *abrupt* could act downstream of ER stress, which may explain why it's upregulated in *Minute* cells (Kucinski et al., 2017). Another possibility is that the lack of effect of p-eIF2α in comparison to GSTGFP could be due to the difference in sensitivity between the two readouts.

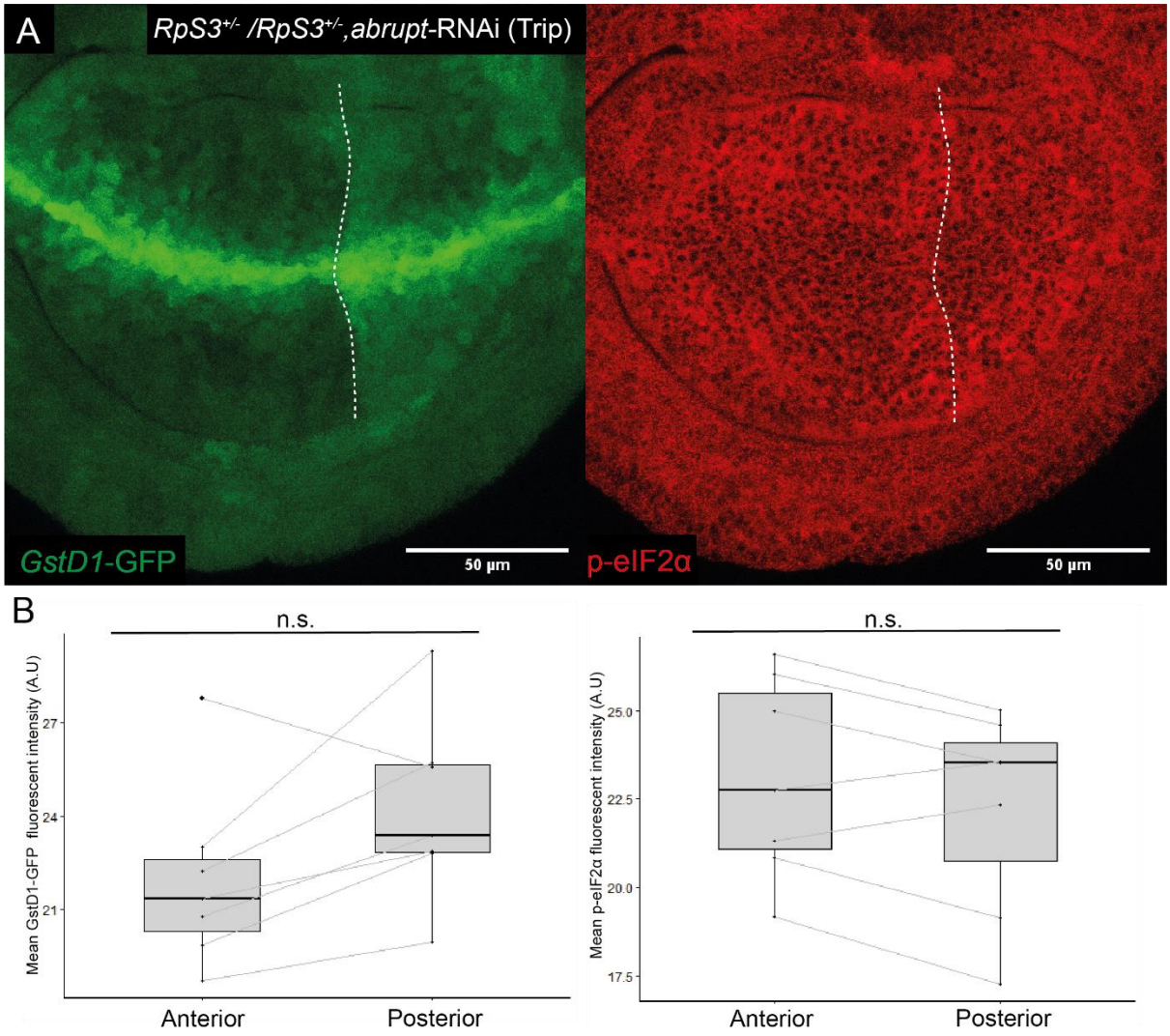

Figure 13: Inhibition of *abrupt* causes a mild upregulation in oxidative stress pathway activation and factors involved in the UPR.

(A) An RpS3$^{+/-}$ wing disc with *abrupt*-RNAi (Trip) specifically expressed in the posterior compartment under a *hedgehog*-GAL4 driver (*hh*-GAL4) and harboring the Nrf2 reporter *GstD1*-GFP (Green) and immunostained for phosphorylated eIF2α (p-eIF2α) (Red). (B) Mean signal intensity of Gst-GFP (Right) and p-eIF2α (Left) between anterior and posterior compartment of wing disc shown in A (Wilcoxon signed Rank test p = 0.078 for both).

4.3 Discussion

The pronounced effects produced by the expression of *abrup*t-RNAi (KK) line in the Nrf2-targeted screening (1.2.2) made it a promising candidate as a potential novel regulator of cell competition. Initial results supported this where the expression of the *abrup*t-RNAi (KK) line in *RpS3*$^{+/-}$ clones substantially increased their rate of elimination by surrounding WT cells (Figure 6). Furthermore, strong upregulation of JNK, p-eIF2α and Nrf2 pathway activation produced by expression of the *abrup*t-RNAi (KK) line (Figure 7 and Figure 8) indicated that, similar to *Minute* mutations, it strongly affects both the UPR and the oxidative stress response. The attenuation of translation observed in *abrup*t-RNAi (KK) most likely occurs downstream p-eIF2α activation, as it is known to shut down translation in response to elevated stress (Hetz et al., 2011). Given how critical the ability to translate is for the viability of a cell it is possible that impaired translation is what drives the cells to be eliminated. It would be interesting to see whether inhibition of eIF2α activation would rescue *abrup*t-RNAi (KK) line expressing cells from elimination. Expression of the key competition factor Xrp1 was also found to be upregulated in *abrup*t-RNAi (KK) line cells, with transcriptional data from qPCR showing Xrp1 expression exceeding levels seen in other loser phenotypes such as *Minutes* (7-fold vs 3-fold). A substantial upregulation of the transposable elements *copia* and *1731* was also observed, suggesting that transposon regulation is impaired, which correlates with transcriptional data from *Minute* cells (Unpublished data). Inhibition of Xrp1 in *abrup*t-RNAi (KK) line expressing cells rescued them from elimination, which suggests that the competitive effects mediated by the *abrup*t-RNAi (KK) line most likely occur upstream of Xrp1.

The strong competitive phenotype produced by the *abrupt*-RNAi (KK) line could however not be reproduced through inhibition of *abrupt* using other RNAi lines or with *abrupt*-mutant strains, leading us to question the validity of the *abrupt*-RNAi (KK) line. Subsequent qPCR analysis revealed the *abrupt*-RNAi (KK) line did not downregulate *abrupt*, which indicated that the effects produced by the RNAi were likely due to an off target.

Sequence homology assays for off targets such as BLAST have been used to locate potential off-targets, but none of the off-target candidates identified using this method have been found to be affected by the *abrupt*-RNAi (KK) line. Another approach would be to measure the transcriptional landscape of *abrupt*-RNAi (KK) line expressing cells through transcriptomic methods such as RNA-sequencing. Although this would reveal the relative expression levels of each gene, showing which genes are differentially expressed, the genetic noise produced by the activation of stress pathways and other factors associated with the phenotype would make it difficult to identify the off target with sufficient specificity. Proteomic analysis of *abrupt*-RNAi (KK) cells could also provide some information but would still be similarly susceptible to noise. Some of the noise could however be filtered out by normalising for the effect of Xrp1 overexpression by analysing Xrp1 overexpressing samples together with *abrupt*-RNAi (KK). Genes differentially expressed between XRP1 overexpressing and abrupt-RNAi (KK) sample datasets could then provide a list of candidates which could then be screened for homology to the *abrupt*-RNAi (KK) hairpin. The most promising candidates could then be expressed or inhibited respective to what effect the *abrupt*-RNAi (KK) to see if it causes an identical phenotype.

Currently it appears the best option to identify the off-target is by continuing the sequence homology approach, although so far candidate genes identified using this method have not been positive hits. Paul Langton recently identified a new potential off-target candidate gene: *Br140* (Bromodomain-containing protein, 140KD) which encodes a component of the ENOK complex, which is associated with the regulation of the cell cycle. Hopefully, this gene will turn out to be the off target, otherwise we will continue our pursuit in hopes of eventually identifying it.

Despite the unfortunate presence of an off-target in the *abrupt*-RNAi (KK) line, it appears Abrupt may still play some role in cell competition as downregulation of *abrupt* using the *abrupt*-RNAi (Trip) line appears to mildly enhance oxidative stress signalling in *Minute* discs. This suggests *Minute* cells may upregulate *abrupt* to cope with elevated levels of stress. It will be important to combine the *abrupt* mutants described with *Minute* mutations to determine whether the enhanced phenotypes observed with the *abrupt*-RNAi (Trip) line can be recapitulated with *abrupt* mutations. Off-target effects are a recurring issue among those who use RNAi lines with many methods developed to identify off targets, although our search for the off-target has been fruitless, by utilising different methods we may be able to identify it.

Interestingly, similar to what we observed in *abrupt*-RNAi (KK) cells, *xrp1* and *copia* have been found to be strongly upregulated in cells expressing a mutated form of Upf2, a factor belonging to the Nonsense Mediated mRNA decay (NMD) pathway. The NMD pathway regulates mRNA degradation in a large portion of the transcriptome, preventing transcription of abrogated and harmful proteins to ensure the viability of the cell (Xu et al., 2019, Mendell et al., 2004). Dysregulation of multiple components of the NMD pathway has also been shown to reduce cell viability and proliferation, where NMD impaired clones show reduced growth when generated in a WT background (Metzstein and Krasnow, 2006, Avery et al., 2011). Much like in *Minute* clones (Li and Baker, 2007), the reduced size of NMD impaired clones could be rescued by expressing the caspase inhibitor: P35 (Avery et al., 2011). This indicates that apoptosis is the primary factor contributing to the reduced clone size of NMD impaired clones, which suggests cell competition may be involved. It would be interesting in the future to test whether NMD impaired clones are subject to cell competition. Later, it was found that the DNA-damage response protein Gadd45 was the primary driver of apoptosis in NMD impaired clones (Nelson et al., 2016). Incidentally, Gadd45 and many other NMD substrates, including Arc1 and Xrp1 are differentially expressed in prospective loser cells (Kucinski et al., 2017, Xu et al., 2019) Given the similarities between *abrupt*-RNAi (KK) clones and NMD impaired clones, it may be worth investigating whether disruptions of the NMD pathway are involved in the phenotype produced by the *abrupt*-RNAi (KK) line.

The substantial activation of JNK observed in *abrupt*-RNAi (KK*)* samples (Figure 7) indicates that Ire1α is likely strongly activated as it acts directly upstream of JNK and other stress response factors such as XBP1 and NFκB in response to misfolded protein accumulation in the ER (Hollien et al., 2009, Hetz et al., 2011). Another process Ire1α takes part in is the regulated Ire1-dependent decay (RIDD) pathway which oversees degradation of accumulating mRNA in the ER, preventing further accumulation of translated proteins in the ER-lumen (Coelho and Domingos, 2014). Investigating whether Ire1α is involved in the phenotype produced by the *abrupt*-RNAi (KK) line may shed further light on how it mediates the loser status.

Interestingly, the NMD pathway has been shown to directly regulate Ire1α as well as other components of the UPR to prevent excessive UPR activation in response to innocuous stress (Karam et al., 2015). Conversely, UPR activation in response to sufficient stress causes the NMD pathway to be downregulated via eIF2α, allowing for a stronger stress response (Karam et al., 2015, Usuki et al., 2019). The close relation of the NMD pathway to cell viability and the UPR suggests it may play a role in cell competition, making it a promising target for future investigation.

4.4 Conclusion

In conclusion, the expression of the *abrupt*-RNAi (KK) line in wild-type cells drives them to become losers. In addition, when expressed in loser cells, the *abrupt*-RNAi (KK) line enhances the loser status driving them to be eliminated at a higher rate. The effects of *abrupt*-RNAi (KK) expression mimics most characteristics of loser cells, such as elevated stress pathway activation, high Xrp1 expression and enhanced border cell death. The loser status mediated by the *abrupt*-RNAi (KK) line can be rescued with Xrp1 inhibition suggesting that the loser status conferred by *abrupt*-RNAi (KK) line is Xrp1 dependent. Despite the unfortunate discovery that the *abrupt*-RNAi (KK) line did not target *abrupt* and that the previous results were due to an off target, the results are still worth investigating and hopefully by identifying the off-target we may find a novel factor associated with cell competition. The function of Abrupt in cell competition remains unclear: clonal inhibition of Abrupt using mutations are not sufficient to induce cell competition yet inhibition of *abrupt* using the *abrupt*-RNAi (Trip) line shows a noticeable trend towards enhanced stress pathway activation. This suggests that *abrupt* may potentially be upregulated in prospective losers in order to counter elevated levels of stress signalling. Further investigation of the effects of *abrupt* inhibition through both Abrupt mutants as well as the *abrupt*-RNAi (Trip) line may shed further light on how Abrupt is involved in competitive processes.

5 Investigating the consequences of Xrp1 overexpression

5.1 Rationale

Previous studies have established the importance of Xrp1 in cell competition, where it has been shown to be required for *Minute* cell competition and many of the signalling changes observed in *Minute* cells (Blanco et al., 2020, Baillon et al., 2018). Due to the established importance of Xrp1 in cell competition, we sought to understand how Xrp1 mediates its competitive effect. To achieve this, we investigated the effect of Xrp1 overexpression in wing discs on readouts of the loser status. Furthermore, by optimising conditions for Xrp1 overexpression we hoped to emulate the levels of Xrp1 expression observed in *Minute* discs to determine whether the levels of Xrp1 upregulation observed in *Minutes* are sufficient to drive WT cells to become losers.

5.2 Results

5.2.1 The function of Xrp1 in cell competition is isoform dependent

Predictions of Xrp1 have suggested that it encodes 7 alternative transcripts, which can be translated to two isoforms; the 668aa Long isoform ($Xrp1^{Long}$) and the 406aa Short isoform ($Xrp1^{Short}$) (Figure 14) (Mallik et al., 2018). We began by measuring levels of Nrf2 activation in discs overexpressing the Long ($Xrp1^{Long}$) and Short ($Xrp1^{Short}$) isoforms of Xrp1 in the posterior compartment with the *en*-GAL4 driver in the presence of *GstD1-GFP*.

When expressed in the posterior compartment, the UAS-$Xrp1^{Short}$ line did not appear to affect Nrf2 activation in any significant manner. Cell death was similarly unaffected when measured via caspase staining. Generating flies overexpressing $Xrp1^{Long}$ under the same conditions proved difficult as it caused lethality before the L3 larval stage, which is when we dissect out wing discs. After several attempts to generate $Xrp1^{Long}$ expressing larvae we designed a condition that yielded viable larvae. This was achieved using the temperature sensitive GAL4 inhibitor: $GAL80^{ts}$. Larvae were raised at 18 °C for 8-9 days during which Xrp1 expression was inhibited, then shifting to 29 °C for 24-hours to induce Xrp1 expression before dissecting. Wing-discs collected from larvae maintained under these conditions were deformed, with the $Xrp1^{Long}$ expressing posterior compartment growing smaller than the anterior. Caspase staining showed high levels of cell death in the $Xrp1^{Long}$ expressing portion of the wing discs. Imaging of *GstD1*-GFP in the wing discs showed a considerable upregulation of Nrf2 activity in the $Xrp1^{Long}$ expressing posterior compartment (Figure 14). Staining for p-eIF2α also revealed an increased activation of proteotoxic stress pathways in Xrp1 overexpressing cells (Figure 15). We pursued the effect of Xrp1 on proteotoxic stress further by staining against Bip, an ER-chaperone which binds to and activates PERK, a ER-membrane bound kinase which acts upstream of eIF2α activation. These immunostainings revealed a noticeable trend towards Bip upregulation (Figure 14), but as only one set of samples was imaged it was not significant. One could speculate that upregulation of Bip would cause more PERK to be activated which in turn would cause an increase in eIF2α phosphorylation.

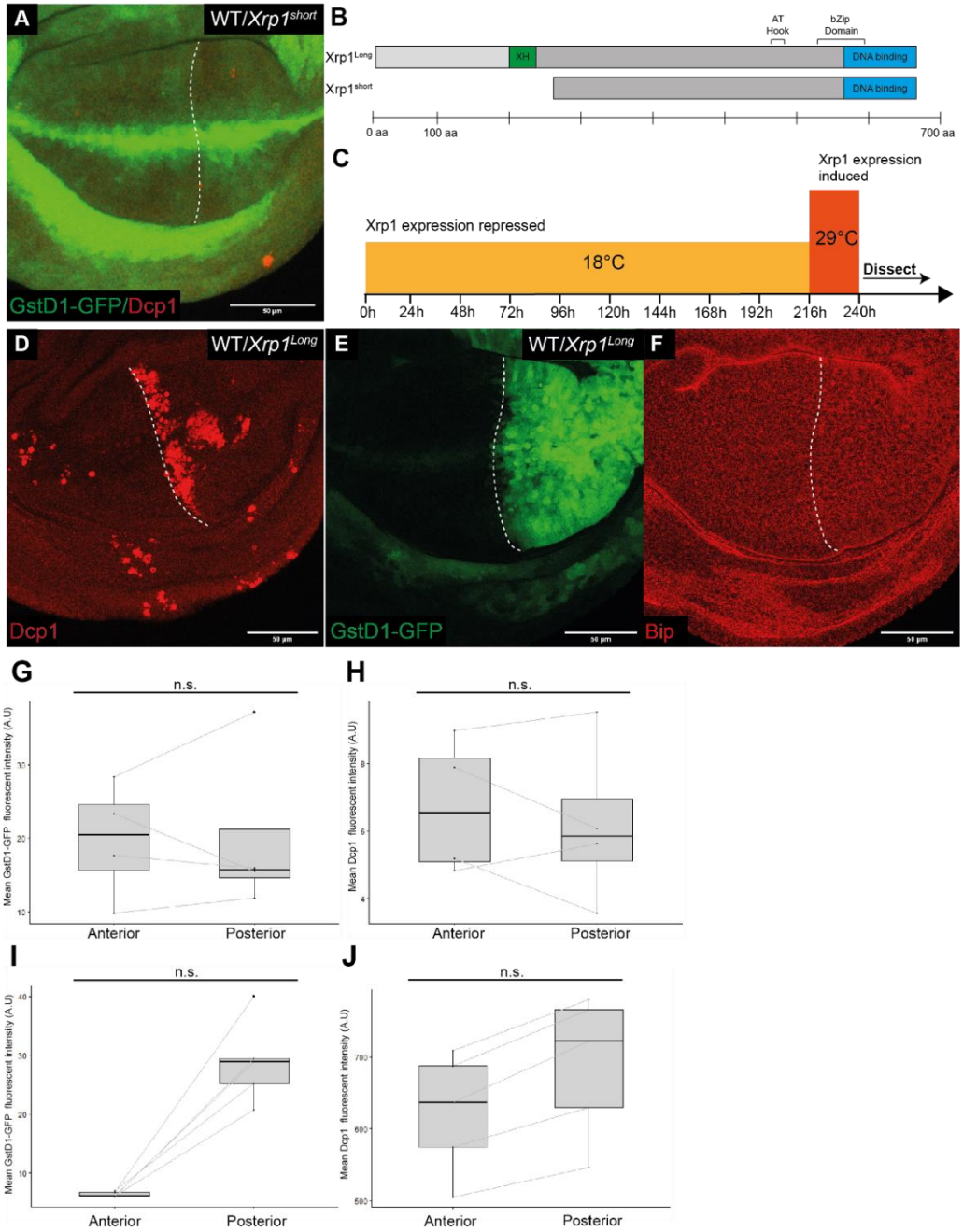

Figure 14: The competitive function of Xrp1 is isoform dependent

(A) A phenotypically WT *Drosophila* wing disc harboring the Nrf2 activation marker *GstD1*-GFP (Green), with the Xrp1^{Short} isoform specifically expressed in the posterior compartment using the *en*-GAL4 driver with immunostaining for Death-Caspase 1 (Dcp1) (Red). (B) Model of the Xrp1 Long (Xrp1^{Long}) and Short (Xrp1^{Short}) isoforms, showing the DNA binding C-terminal domain DNA binding domain in blue (aa 565-668 in the Long isoform) as well as the more amino-terminal conserved sequence (XH) in Green (aa 189-234 in Long isoform). Likely locations for AT-hook and bZip domain indicated. Schematic was adapted from figure by Blanco and colleagues (Blanco et al., 2020). (C) Schematic representation of conditions for the generation of Xrp1^{Long} expressing wing discs. (D) A wing disc with the Xrp1^{Long} isoform expressed in the posterior compartment stained for Dcp1. (E,F) Wing disc of the same genotype as shown in D, showing *GSTD1-GFP* (Green, E) and immunostained for Bip (Red, F). (G-J) Mean signal intensity of Gst-GFP (Right) and Dcp1 (Left) between anterior and posterior compartments of wing discs shown in A-F. (G-H) Quantified signal of Xrp1^{Short} wingdisc shown in A (G) GstD1-GFP (4 technical repeats, Wilcoxon signed Rank test p = 0.88), (H) Dcp1 (4 technical repeats, Wilcoxon signed Rank test p = 0.88). (I) Quantified GstD1-GFP signal in Xrp1^{Long} wingdisc shown in E-F (5 technical repeats, Wilcoxon signed Rank test p = 0.06). (J) Quantified Dcp1 signal in Xrp1^{Long} wingdisc shown in D (5 technical repeats, Wilcoxon signed Rank test p = 0.06).

We also used the polyubiquitin-specific antibody: FK2, to stain against polyubiquitinated proteins to measure relative levels of ubiquitinated protein aggregates between compartments. The FK2 staining produced a strong signal in the posterior Xrp1^{Long} expressing compartment of the wing disc while the anterior compartment retained a relatively low signal (Figure 15). This suggested that Xrp1 overexpressing cells have more protein aggregates, which may explain why proteotoxic stress pathways are activated at higher levels in those cells.

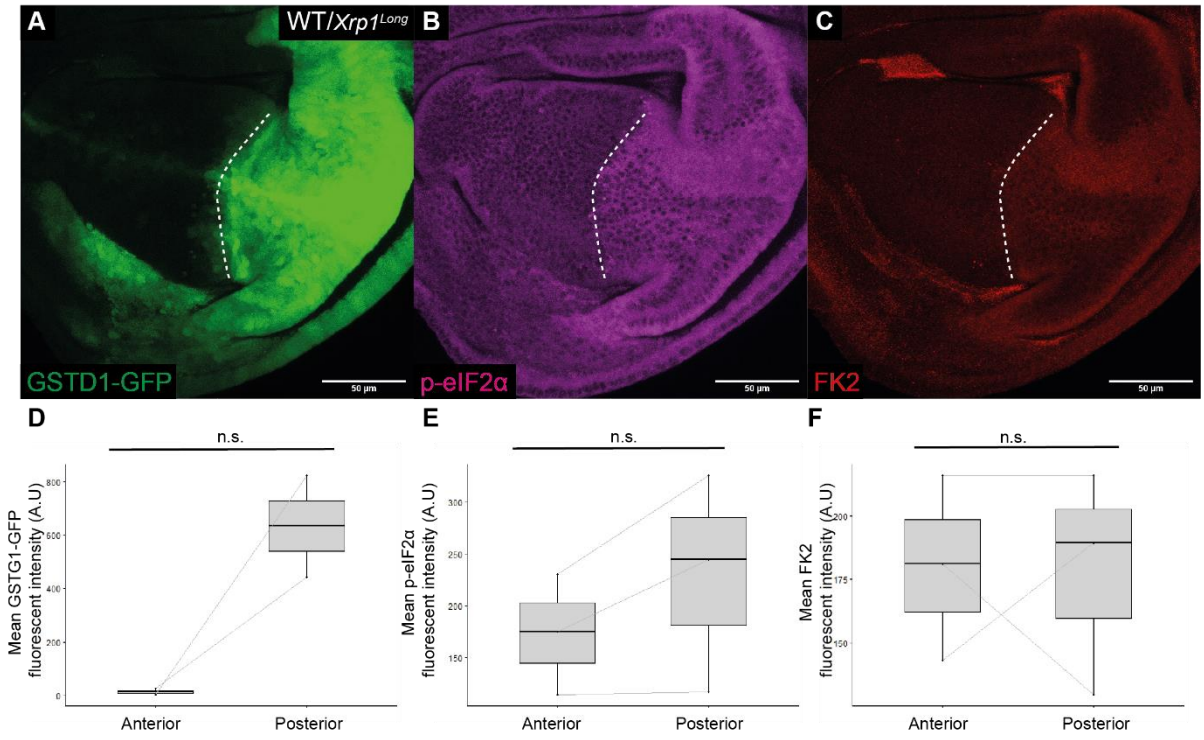

Figure 15: Overexpression of the Xrp1^{Long} isoform causes an accumulation of misfolded proteins and enhances UPR signaling.

(A) WT wing discs harbouring the Nrf2 reporter *GstD1*-GFP (Green), with Xrp1^{Long} isoform overexpressed in the posterior compartment under the *engraile*d-GAL4 driver. The Anterior/Posterior boundary marked with a white dotted line. (B) Immunostaining for p-eIF2α (Magenta). (C) Immunostaining for poly-ubiquitinated misfolded proteins via FK2 antibody (Red). (D-E)) Mean signal intensity between anterior and posterior compartment of wing discs shown in A-C for (D) GST-GFP (2 technical repeats, Wilcoxon signed Rank test p = 0.5), (E) p-eIF2α (3 technical repeats, Wilcoxon signed Rank test p = 1), (F) FK2 (3 technical repeats, Wilcoxon signed Rank test p = 0.25).

To determine if similar results could be produced by overexpressing Xrp1 using independent lines, we generated a cross expressing an extra copy of Hemagglutinin- (HA) tagged Xrp1^{Long} (Xrp1^{HA}) in the posterior compartment of a wing disc (Figure 16). Consistent with the expression of Xrp1^{Long} line, severe cell death could be observed in the Xrp1^{HA} expressing posterior compartment. There was also a strong *GstD1*-GFP signal indicating enhanced Nrf2 activation in Xrp1^{HA} over-expressing cells. Xrp1^{HA} could be visualised via anti-HA-tag antibody and anti-HA staining confirmed that Xrp1^{HA} was exclusively expressed in the posterior compartment (Figure 16).

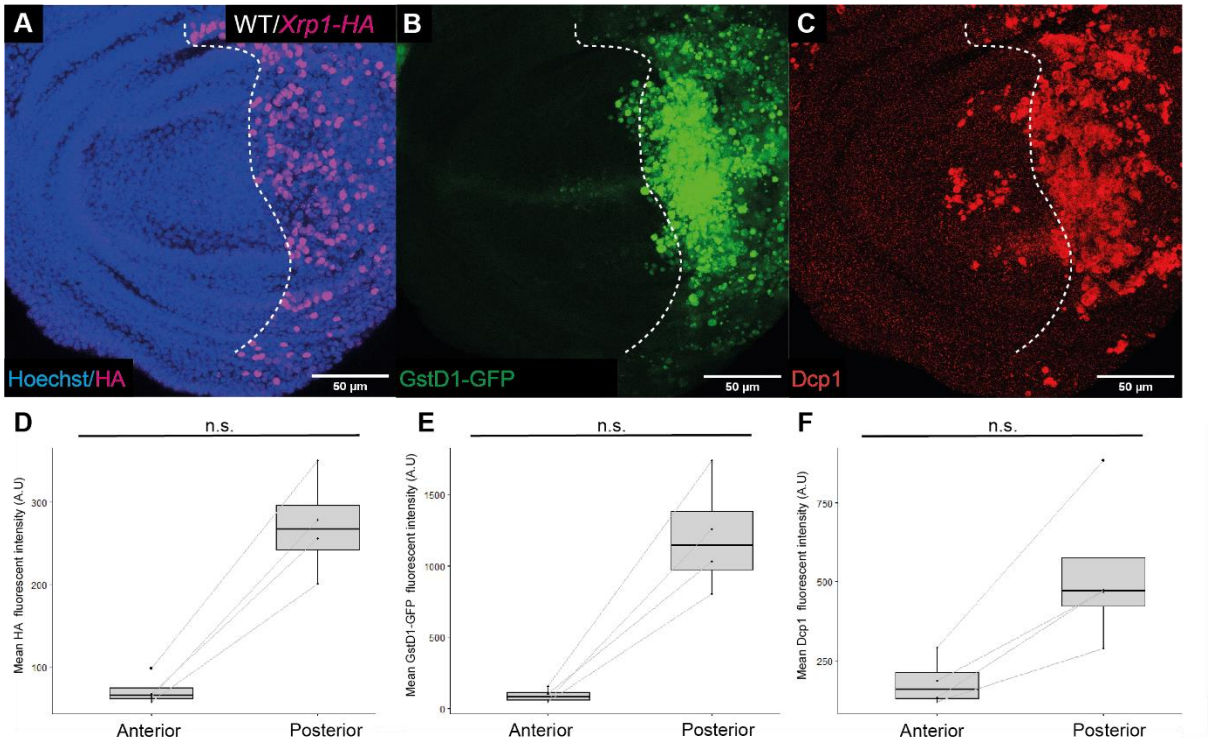

Figure 16: Overexpression of Xrp1 tagged with HA (Xrp1-HA) triggers the oxidative stress response and drives cell death.

WT wing disc harbouring the Nrf2 reporter: *GstD1*-GFP (Green) and overexpressing haemagglutinin (HA)-tagged Xrp1 (Xrp1-HA) in the posterior compartment under the *engrailed*-GAL4 driver (*en*-GAL4). (A) HA antibody staining labelling the expression of Xrp1-HA in disc (Magenta), with Hoechst nuclear labelling (Blue). (B) Nrf2 activity labelled with GstD1-GFP (green). (C) Cell death measured via Death caspase-1 (Dcp1) staining (red). (D-F) Mean signal intensity between anterior and posterior compartment of wing disc shown in A-C for (D) HA (4 technical repeats, Wilcoxon signed Rank test p = 0.12), (E) GSTD1-GFP (4 technical repeats, Wilcoxon signed Rank test p = 12), (F) Dcp1 (4 technical repeats, Wilcoxon signed Rank test p = 0.12).

5.2.2 Inhibition of Irbp18 mildly rescues *Minutes* from stress

Recent studies have identified the bZip protein Irbp18, a common binding partner of Xrp1, as a key regulator of cell competition and its inhibition rescued *Minute* clones from elimination (Blanco et al., 2020). This correlates with preliminary RNA-sequencing data where Irbp18 was found to be upregulated in several loser genotypes (Kucinski et al., 2017). Another common binding partner of Irbp18 is the Activating Transcription Factor 4 (ATF4), which is involved in the UPR (see Figure 3) (Reinke et al., 2013). However, unlike Xrp1, overexpression of Irbp18 its own does not appear to be sufficient to confer the loser status (Blanco et al., 2020). This may be due to lack of Xrp1 to interact with excess Irbp18 in Irbp18 overexpressing cells (Blanco et al., 2020) Given that Irbp18 inhibition was found to rescue competition, we sought to determine whether it would also reduce proteotoxic stress in *Minutes*. We began by testing an *irbp18-RNAi* line to determine whether downregulation of *irbp18* would affect stress pathway activation. The *irbp18-RNAi* line was expressed under a *hh-GAL4* driver in a $RpS3^{+/-}$ disc carrying the *GSTD1*-GFP reporter and stained against p-eIF2α. Although the effects of the Irbp18 knockdown were faint, we could detect significantly lower levels of *GSTD1*-GFP and p-eIF2α signal in the posterior compartment (Figure 17). We speculated that the RNAi did not sufficiently inhibit Irbp18 to produce a strong rescue. Later, an identical experiment performed by Paul using another RNAi line produced a strong downregulation of both *GSTD1*-GFP and p-eIF2α in *Minute* discs, suggesting that, like Xrp1, Irbp18 acts as an upstream regulator of both Nrf2 and p-eIF2α.

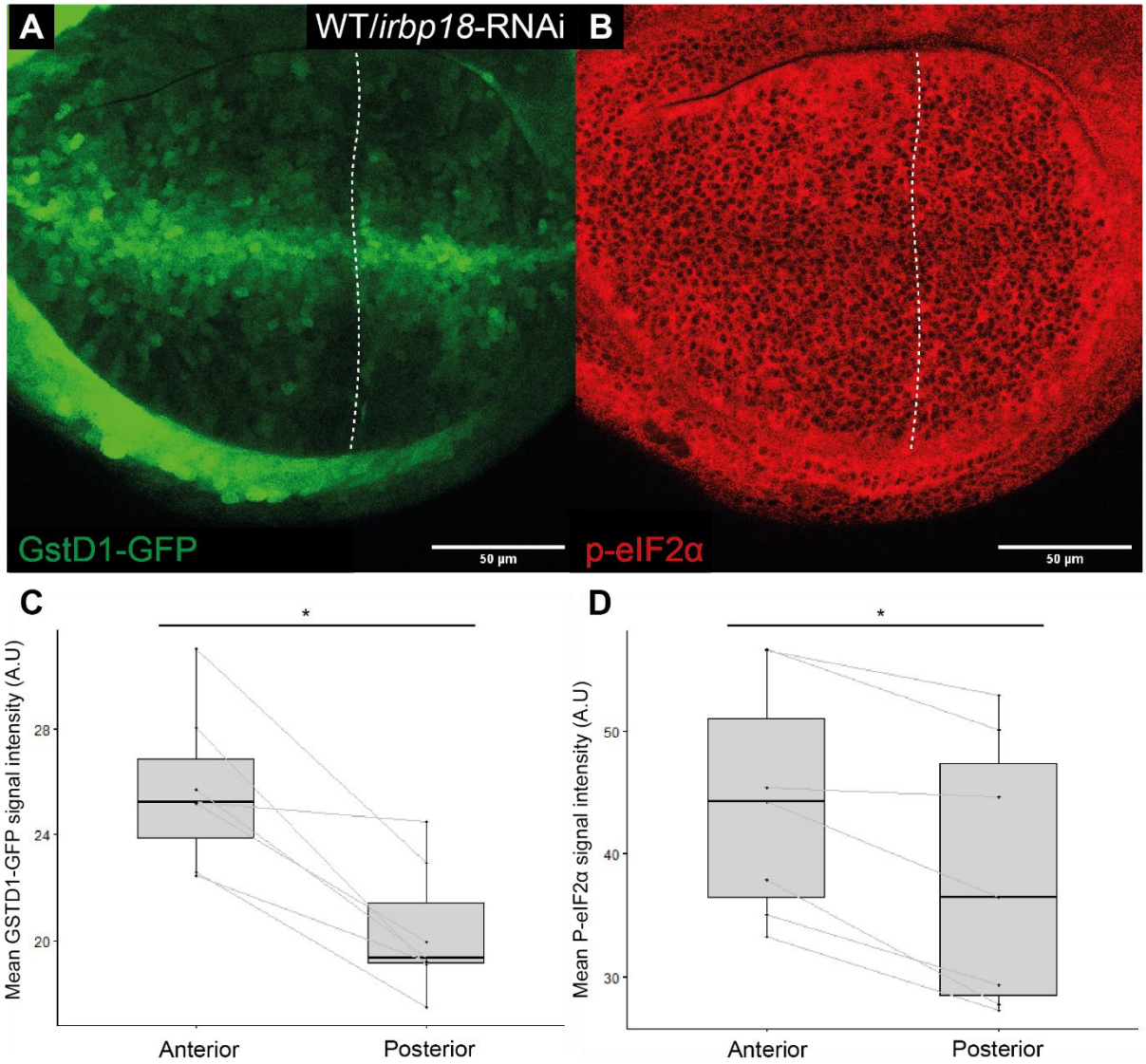

Figure 17: Inhibition of Irbp18 causes a mild rescue of the oxidative stress response pathways and Unfolded protein response in *Minutes*.

Irbp18 was inhibited via RNAi (*irbp18*-RNAi) in the posterior compartment of *RpS3*$^{+/-}$ wing ubiquitously expressing the Nrf2 reporter *GstD1-GFP* (Green), Anterior/Posterior compartment boundary marked with a white dotted line. (A) *GstD1-GFP* signal. (B) UPR activation measured via p-eIF2α antibody (Red). (C) Quantification of *GstD1-GFP* signal intensity between anterior and posterior compartments (7 technical repeats, Wilcoxon signed Rank test p = 0.002). (D) Quantification of p-eIF2α signal intensity between anterior and posterior compartments (7 technical repeats, Wilcoxon signed Rank test p = 0.002).

5.3 Discussion

The stark difference between the effects of overexpression of the $Xrp1^{Long}$ and $Xrp1^{Short}$ isoforms on pathways associated with competition (Figure 14 & Figure 15) is likely due to a functional difference between the two isoforms. It is possible that the extra 262 amino acids encoded in the $Xrp1^{Long}$ isoform are necessary for the competitive function of Xrp1 as previous studies have found that the $Xrp1^{Long}$ isoform interacts with significantly larger number of proteins than the $Xrp1^{short}$ isoform (Mallik et al., 2018). Interestingly, protein interaction data of the two isoforms shows that only the Long isoform interacts with the common Xrp1 binding partner: Irbp18 (Mallik et al., 2018). What causes the functional difference between the Long and Short isoforms could be an interesting subject to pursue further. Mutations or deletions within the extra 262 amino acid region of the $Xrp1^{Long}$ isoform might help in this regard, but it would also be interesting to see whether overexpression of those 262 amino acids on their own would be able to reproduce the $Xrp1^{Long}$ overexpression phenotype. Conversely these 262 amino acids might also function as competitive inhibitors of $Xrp1^{Long}$ heterodimerization to Irbp18, thus recuing cells from the loser status.

Recent publications have found that Irbp18 and Xrp1 positively regulate each other and are mutually dependent for their function in cell competition (Blanco et al., 2020). The mild rescue of stress pathways produced by the *irbp18-RNAi* in a *Minute* background (Figure 17) suggests that Irbp18 is also involved in stress pathway activation. As RNAi often results in partial gene knockdown it is possible that the RNAi did not inhibit Irbp18 to sufficient levels to produce a strong rescue. It is also possible that stress pathways are being upregulated in *Minute* cells in an Irbp18 independent manner. It is worth noting that while Irbp18 has the mammalian orthologue: CAAT/Enhancer Binding Protein β (C/EBPγ) (Blanco et al., 2020) Xrp1 has no known mammalian orthologue (Akdemir et al., 2007). C/EBPγ, much like its *Drosophila* orthologue plays an important role in stress response networks through heterodimerization with ATF4 (Huggins et al., 2015).

Several orthologues were recently discovered for Xrp1 within dipteran insects, but orthologues outside of dipteran insects have yet to be identified, likely due rapid divergence through natural selection (Blanco et al., 2020). Although it is unknown whether a mammalian orthologue for Xrp1 exists, the DNA Damage Induced Transcript 3 (DDIT3) encodes the C/EBP homologous protein (CHOP) which shares some functional similarities Xrp1 (Blanco et al., 2020). This includes heterodimerization with C/EBPγ (the mammalian orthologue of Irbp18) as well as function in both regulation of apoptosis and the DNA-damage response. Furthermore, ectopic expression of hDDIT3 in developing *Drosophila* eye discs, much like Xrp1, caused a reduction in eye size which could be rescued via the co-expression of an Irbp18-RNAi (Blanco et al., 2020). CHOP also plays an important role in the mammalian UPR (Figure 3), where it acts downstream of ATF4 and PERK to dephosphorylate eIF2α via activation of Gadd43 (Rozpedek et al., 2016). There exists no *Drosophila* orthologue for hDDIT3, but given it's close relation to Xrp1 associated pathways, it is possible that there is some relation between the two (Blanco et al., 2020). It would be interesting in the future to investigate interactions between hDDIT3 and C/EBPγ in mammalian models. For example, observing whether CHOP overexpression in mammalian cells is sufficient to confer the loser status would be a good start. This could then be followed up by inhibiting C/EBPγ in CHOP overexpressing cells to measure it's effect. Transcriptional comparison of both mammalian and *Drosophila* CHOP overexpressing to *Drosophila* XRP1 overexpressing cells (and even secondary sets where C/EBPγ/Irbp18 is inhibited) might shed light on the functional similarities between CHOP and Xrp1.

The elevated levels of cell death of $Xrp1^{long}$ overexpression (Figure 14) could be reproduced via $Xrp1^{HA}$ overexpression (Figure 16) and with anti HA-tag staining we could monitor the frequency of cell death in $Xrp1^{HA}$ expressing cells. Furthermore, the HA-tag staining may also open up the possibility of viewing the subcellular localization of Xrp1 in Xrp1-HA overexpressing cells. The anti-HA staining however displayed some variance in signal intensity to which I responded by lowering the laser emission in the confocal microscope, this however led to the loss of some of signal of the anti-HA staining. When this experiment is repeated, imaging methods will have to be optimised to ensure complete capture of the signal produced by anti-HA immunostainings. The differential expression of $Xrp1^{HA}$ between cells is however interesting, perhaps prolonged $Xrp1^{HA}$ overexpression leads to some compensatory inhibition within cells causing younger cells to exhibit lower levels of expression. It would be interesting to observe the effect of co-expression of *irbp18*-RNAi with either Xrp^{Long} or $Xrp1^{HA}$ to see whether it rescues competition and stress pathway activation.

5.4 Conclusion

In conclusion, these results, along with research by other groups show clearly that Xrp1 along with Irbp18 play important role in cell competition by affecting both cell survival and stress pathways. Only the long isoform of Xrp1 displays competitive phenotypes when overexpressed, possibly due to its ability to interact with Irbp18. Stress signalling is strongly affected by Xrp1 overexpression with enhanced stress pathway activation, accumulation of misfolded proteins (measured via FK2 antibody) and Bip upregulation. Similar effects can be produced via expression of $Xrp1^{HA}$ which with anti-HA immunostaining showed that elevated levels of cell death and Nrf2 activation correlating with regions of $Xrp1^{HA}$ expression.

6 PERK inhibition

6.1 Rationale

As many loser mutants have elevated levels of proteotoxic stress, we sought to further our understanding of what drives these changes and how they may influence progression to the loser status. This was especially visible in $Xrp1^{Long}$ overexpressing cells, which displayed elevated levels of misfolded proteins and activation of components of the UPR. In our previous experiments we have primarily used the eIF2α activation as a marker for proteotoxic stress; eIF2α belongs to the PERK branch of the proteotoxic stress response pathways in the cell, which when activated triggers translation inhibition and activation of ATF4, which mediates the ER-stress response by inducing chaperone gene expression and pro-apoptotic genes that lead to apoptosis upon sustained ER-stress. By inhibiting PERK, we would effectively inhibit eIF2α activation allowing us to observe how it influences the fitness of the cell. Investigating the function of PERK in cell competition was therefore an attractive prospect to gain insight into what drives ER-stress pathway activation in *Minute* and other loser status inducing mutations.

6.2 Results

We began by testing the effects of PERK inhibition in *Minute* discs. PERK is a membrane bound kinase which is responsible for the phosphorylation of both Nrf2 and eIF2α, so based on that information we hypothesised that by inhibiting PERK we would see a rescue of p-eIF2α upregulation and Nrf2 activation in *Minute* wing discs. Using a *hh*-GAL4 driver we expressed two *PERK-RNAi* lines (HMS and KK*)* in the posterior compartment of $RpS3^{+/-}$ wing discs with the *GstD1-GFP* reporter in the background (Figure 18). Quantifying images of these wing discs stained with p-eIF2α antibody showed a significantly reduced levels of p-eIF2α in the posterior compartment of wing discs with both RNAi lines, however *GstD1-GFP* signal remained unchanged between compartments (Figure 18). This bears similarity to a previous experiment where overexpression of Gadd34, the phosphatase of p-eIF2α caused a similar reduction of p-eIF2α, but unlike the *PERK*-RNAi lines, Gadd34 overexpression also caused a significant upregulation of Nrf2 activity (Takeuchi, 2019). The lack of effect on Nrf2 activity came as a surprise as Nrf2 activation occurs directly downstream PERK activation. It is likely that the RNAi line used led to a incomplete knockdown, and the remaining PERK protein is sufficient to phosphorylate Nrf2. The fact that Nrf2 activity did not decrease with reduced levels of p-eIF2α indicates that inhibition of eIF2α activity does not aid the fitness of a cell. It is also possible that Nrf2 is being activated through PERK-independent pathways. Reduced eIF2α activity prevents translational inhibition, which in turn causes more misfolded proteins to be transcribed. This in turn would cause an increased accumulation of misfolded proteins in the ER, enhancing ER-stress (Hetz et al., 2011). Thus, although translational inhibition may not be beneficial for the viability of the cell, in the context of elevated ER-stress it is.

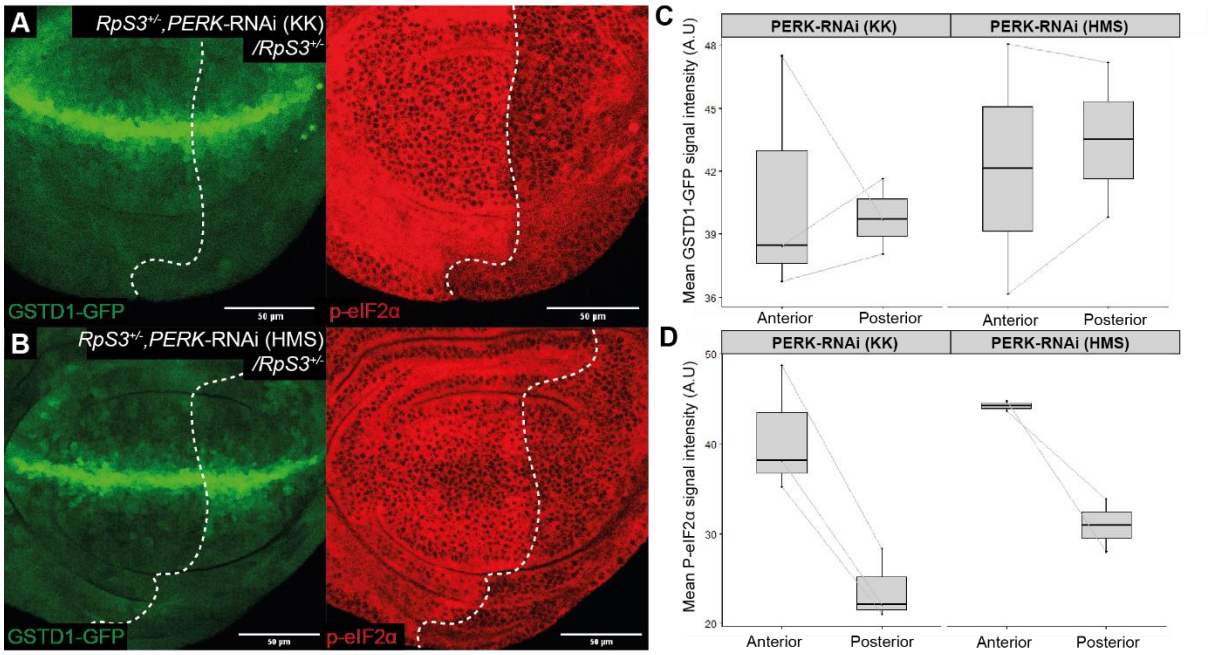

Figure 18: PERK inhibtion rescues *RpS3*$^{+/-}$ cells from hyperactivation of the UPR but has no significant effect on the oxidative stress response.

(A) *Minute* (RpS3$^{+/-}$) wing discs carrying the Nrf2 marker *GSTD1*-GFP (Green) with posterior compartment specific expresison of PERK-RNAi (KK) line (110278) expressed under the *hedgehog*-GAL4 (*hh*-GAL4) driver, immunostained for p-eIF2α (Red). (B) *Minute* (RpS3$^{+/-}$) wing discs carrying the Nrf2 marker *GSTD1*-GFP (Green) with posterior compartment specific expresison of PERK-RNAi (HMS) line (35162) expressed under the *hedgehog*-GAL4 (*hh*-GAL4) driver, immunostained for p-eIF2α (Red). (C) Quantification of mean signal intensity of *GstD1*-GFP in *PERK*-RNAi line expressing RpS3$^{+/-}$ wing discs (p = 1), as illustrated in A and B. (D) Quantification of mean signal intensity of p-eif2α in *PERK*-RNAi expressing *RpS3*$^{+/-}$ wing discs as illustrated in section A and B. PERK-RNAi (HMS): (p = 0.25), PERK-RNAi (KK): (p = 0.25).

As the *PERK-RNAi* (KK) line showed a stronger rescue of p-eIF2α in *Minute* discs we preferentially used that RNAi line for follow-up experiments as we assumed that it downregulated *PERK* with greater efficiency than the *PERK-RNAi* (HMS) line. Immunostainings of another set of wing discs of the same genotype as the previous experiment with Dcp1 did not show any effect on cell death, but p-JNK immunostaining showed a mild increase in levels of JNK activation in the *PERK-RNAi* expressing posterior compartment (Figure 19). Only a single sample set was stained with Dcp1 and p-JNK, so quantifications of both experiments did not reach the p-value threshold to be considered statistically significant. The quantifications did however show a noticeable trend towards a p-JNK upregulation in the PERK-RNAi expressing posterior compartment.

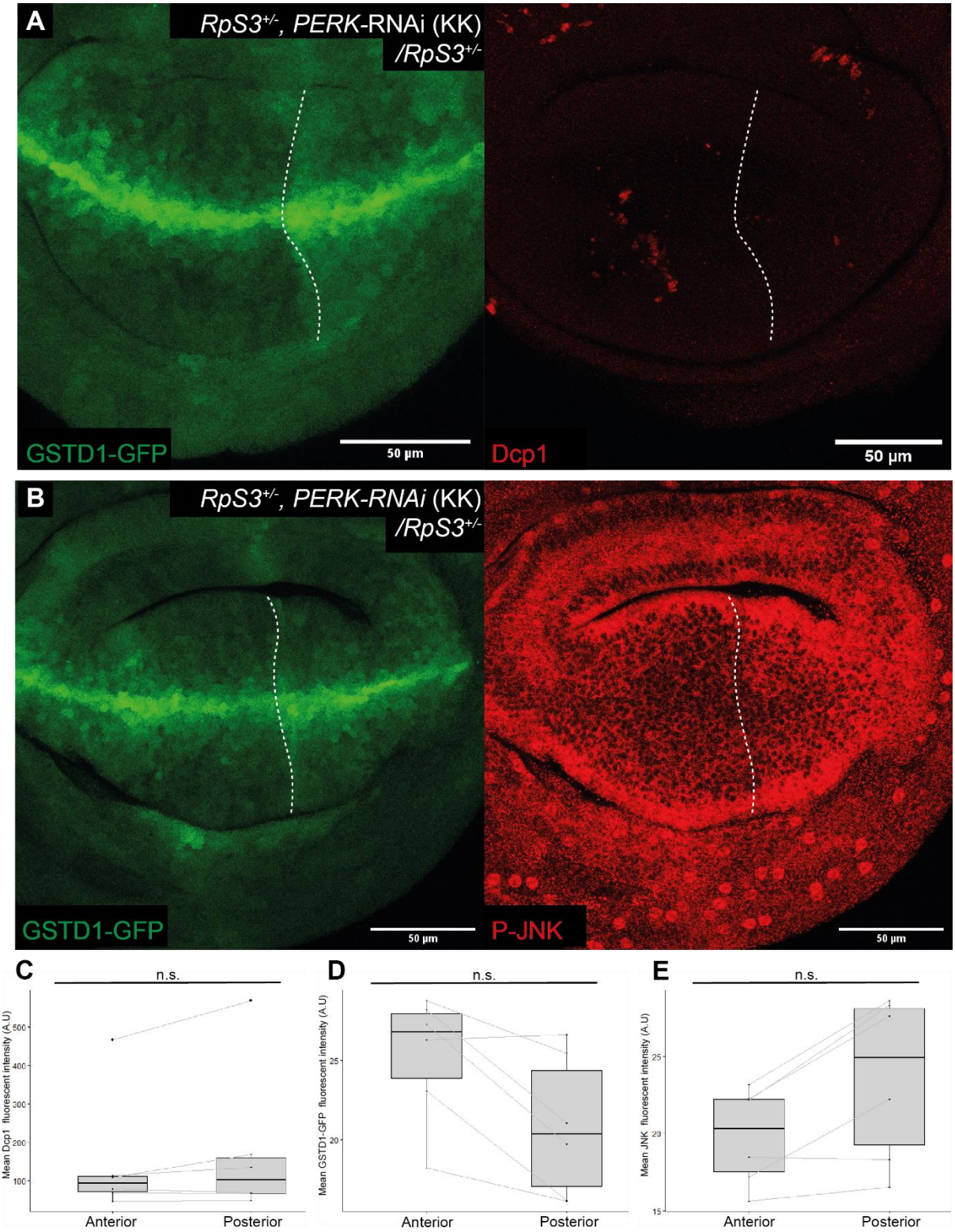

Figure 19: Inhibition of PERK does not affect cell death in *Minute* discs, but shows a trend towards elevated JNK activation.

(A) *Minute* ($RpS3^{+/-}$) wing discs harbouring the Nrf2 marker *GstD1*-GFP (Green) with posterior compartment specific expresison of PERK-RNAi (KK) line under the *hedgehog*-GAL4 (*hh*-GAL4) driver and stained for death caspase 1 (Dcp1) (Red). (B) Similar disc as described in A, stained for phosphorylated JNK (p-JNK) (Red). (C-E) Mean signal intensity between anterior and posterior compartment of wing disc shown in A and B for (C) Dcp1 in wing discs in A (Wilcoxon signed Rank test p = 0.31), (D) GSTD1-GFP in Wing discs in B (Wilcoxon signed Rank test p = 0.06), (E) Dcp1 in wing discs in B (Wilcoxon signed Rank test p = 0.06).

6.3 Discussion

The pronounced rescue of eIF2α phosphorylation produced by both *PERK*-RNAi lines (Figure 18) confirmed that the RNAi-lines were functional. Further confirmation could be acquired later by measuring the relative expression of *PERK* in *PERK*-RNAi wing discs via qPCR. Such measurements could also confirm whether the difference in p-eIF2α rescue between the two RNAi lines is due to differing levels of PERK inhibition. Although several kinases are capable of phosphorylating eIF2α, PERK kinase activity is primarily mediated by ER-stress which tends to be high in prospective loser (Pakos-Zebrucka et al., 2016, Kucinski et al., 2017). Given that the majority of p-eIF2α signal was rescued via PERK inhibition, the unfolded protein response and PERK are likely the primary drivers for p-eIF2α accumulation in ribosomal mutants and potentially other prospective losers. The lack of effect on Nrf2 activation raised questions as we had expected the *PERK*-RNAi to cause a reduction in *GstD1*-GFP levels. As RNAi does not completely quench the expression of its target, we speculated whether the remaining levels of *PERK* expression were sufficient to retain Nrf2 activation. Another possibility is that Nrf2 activation is also mediated through other pathways, independent of PERK, potentially through Glycogen Synthase Kinase 3β (GSK-3β) (Shaggy (Sgg) in *Drosophila*), which has been shown to activate PERK directly (Culbreth and Aschner, 2018).

Some research has suggested that PERK is capable of mediating JNK activation in an ATF4 dependent manner (Demay et al., 2014), furthermore, previous studies performed by our lab found JNK activation to occur downstream translation inhibition, which is mediated by one of PERKs downstream targets: p-eIF2α (Dinan, 2018). Based on these findings, one would have expected reduced levels of JNK in *PERK*-RNAi expressing cells, instead of the mild upregulation observed (Figure 19).

One potential explanation is that, while inhibition of the PERK reduces stress signalling downstream of that specific branch of the UPR, it does not alleviate the cells from ER-stress. The inhibition of PERK may therefore cause increased signalling through other branches of the UPR to compensate for the accumulation of misfolded proteins in the ER. This would include the Ire1α branch of the UPR which acts directly upstream JNK activation (Urano et al., 2000). It would be informative to investigate Ire1α and its targets in future experiments involving PERK inhibition. Cell death was not significantly affected by PERK inhibition in the posterior compartment of *Minute* discs; however, competition is known not to occur across the A-P boundary. Expressing *PERK-RNAi* in *Minute* clones would allow us to measure whether PERK inhibition affects border cell death and competition in heterogenous tissue. Expressing *PERK-RNAi* in *Minute* clones using the MiWo tool, may to some extent rescue the rate of loser cell elimination. Furthermore, it would be interesting to see whether clonal expression of *PERK-RNAi* in a $RpS3^{+/-}$ background would cause $RpS3^{+/-}$, *PERK-RNAi* expressing cells to outcompete their $RpS3^{+/-}$ neighbours.

6.4 Conclusion

The inhibition of PERK in prospective loser cells via two separate RNAi lines causes a rescue of eIF2α activation, potentially alleviating them from downstream effects such as translational inhibition. However, PERK inhibition did not affect activation of the oxidative stress response, where Nrf2 activity remained unchanged. This suggests that either a small amount of PERK transcription is sufficient to maintain Nrf2 activity, or that PERK independent pathways for Nrf2 phosphorylation exist. An increase in JNK activity could be observed in PERK inhibited cells, potentially through a downstream effect of mis-folded protein accumulation in the ER-lumen causing increased signalling through other branches of the UPR. In the future will be interesting to see whether PERK inhibition is sufficient to rescue *Minute* clones from elimination by neighbouring WT cells.

7 General discussion

Cell competition is a complex subject affected by a myriad of different factors, as was demonstrated in this thesis, where even a simple off-target can produce a strong competitive phenotype (Figure 6). It also demonstrates that while the concept of cell competition is relatively old, there are still many horizons left to explore. While the off-target of the abrupt-RNAi (KK) line remains unknown, it is likely an upstream effector of Xrp1 (Figure 20) due to the high levels of upregulations recorded (Figure 8 & Figure 12) and the fact that the phenotype could be rescued via Xrp1 inhibition (Figure 9). In the future it will be interesting to pursue the off-target and its link to Xrp1.

Xrp1 is clearly a mediator of cell competition, where its loser phenotype was so strong it was difficult to produce viable Xrp1 overexpressing cells. The isoform dependency of Xrp1 highlights the importance of Irbp18 in its competitive function as the short isoform of Xrp1 was unable to produce any competitive phenotype (Figure 14), most likely to its inability to heterodimerize with Irbp18. Future analysis of the 262 amino acids which separate the Long and Short isoforms may confirm whether that is the case. The noticeable increase in misfolded proteins in Xrp1 overexpressing cells (Figure 15) explains why components of the UPR are affected. It would be interesting in the future to see whether ER-stress can be rescued with either, Xrp1or Irbp18 inhibition.

The inhibition of Irbp18 via RNAi somewhat alleviated *Minute* cells from Nrf2 and p-eIF2α activation (Figure 17). Later inhibition with a stronger RNAi line confirmed that Irbp18 strongly rescues loser cells from Nrf2 and p-eIF2α (unpublished), but Irbp18 overexpression is not sufficient to confer the loser status. Despite producing a significant rescue of p-eIF2α in *Minutes*, PERK inhibition was not sufficient to rescue them from Nrf2 activation or cell death (Figure 18). Later, clonal inhibition of PERK (unpublished) in *Minutes* was also not sufficient to rescue them from elimination, suggesting that Nrf2 is activated, and mediates the loser status independently of PERK.

Research into the subject of cell competition has come far since its discovery over 40 years ago and has in the process become substantially more complex. In *Drosophila*, Xrp1 appears to be the primary driver of cell competition, functioning upstream of both Nrf2 and ER-stress (Figure 12) but understanding how this translates to mammals, and finally humans will be a challenge for the future.

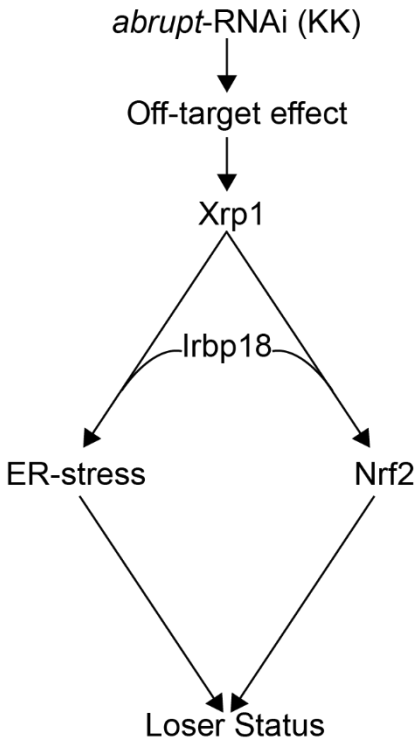

Figure 20: Proposed model for how abrupt-RNAi (KK) line confers the loser status.

The *abrupt*-RNAi somehow indirectly, through an off-target effect, mediates strong upregulation of Xrp1. Xrp1 heterodimerizes with Xrp1 and activates Nrf2, and mediates ER-stress. Factors downstream of ER-stress and Nrf2 then mediate the loser status.

8 References

AKDEMIR, F., CHRISTICH, A., SOGAME, N., CHAPO, J. & ABRAMS, J. M. 2007. p53 directs focused genomic responses in Drosophila. *Oncogene,* 26**,** 5184-5193.

AKIEDA, Y., OGAMINO, S., FURUIE, H., ISHITANI, S., AKIYOSHI, R., NOGAMI, J., MASUDA, T., SHIMIZU, N., OHKAWA, Y. & ISHITANI, T. 2019. Cell competition corrects noisy Wnt morphogen gradients to achieve robust patterning in the zebrafish embryo. *Nature Communications,* 10**,** 4710-4710.

AVERY, P., VICENTE-CRESPO, M., FRANCIS, D., NASHCHEKINA, O., ALONSO, C. R. & PALACIOS, I. M. 2011. Drosophila Upf1 and Upf2 loss of function inhibits cell growth and causes animal death in a Upf3-independent manner. *RNA (New York, N.Y.),* 17**,** 624-638.

BAILLON, L., GERMANI, F., ROCKEL, C., HILCHENBACH, J. & BASLER, K. 2018. Xrp1 is a transcription factor required for cell competition-driven elimination of loser cells. *Scientific Reports,* 8**,** 17712.

BAKER, N. E., KIPARAKI, M. & KHAN, C. 2019. A potential link between p53, cell competition and ribosomopathy in mammals and in Drosophila. *Developmental Biology,* 446**,** 17-19.

BEJARANO, F., BORTOLAMIOL-BECET, D., DAI, Q., SUN, K., SAJ, A., CHOU, Y.-T., RALEIGH, D. R., KIM, K., NI, J.-Q., DUAN, H., YANG, J.-S., FULGA, T. A., VAN VACTOR, D., PERRIMON, N. & LAI, E. C. 2012. A genome-wide transgenic resource for conditional expression of Drosophila microRNAs. *Development (Cambridge, England),* 139**,** 2821-2831.

BITEAU, B., HOCHMUTH, C. E. & JASPER, H. 2011. Maintaining tissue homeostasis: Dynamic control of somatic stem cell activity. *Cell Stem Cell,* 9**,** 402-411.

BLANCO, J., COOPER, J. C. & BAKER, N. E. 2020. Roles of C/EBP class bZip proteins in the growth and cell competition of Rp ('Minute') mutants in Drosophila. *eLife,* 9**,** e50535.

BRIDGES, C. B. & MORGAN, T. H. 1923. *The third-chromosome group of mutant characters of Drosophila melanogaster,* Washington, Carnegie Institution of Washington.

BRODSKY, M. H., WEINERT, B. T., TSANG, G., RONG, Y. S., MCGINNIS, N. M., GOLIC, K. G., RIO, D. C. & RUBIN, G. M. 2004. Drosophila melanogaster MNK/Chk2 and p53 regulate multiple DNA repair and apoptotic pathways following DNA damage. *Molecular and Cellular Biology,* 24**,** 1219-1231.

CLAVERÍA, C., GIOVINAZZO, G., SIERRA, R. & TORRES, M. 2013. Myc-driven endogenous cell competition in the early mammalian embryo. *Nature,* 500**,** 39-44.

COELHO, D. S. & DOMINGOS, P. M. 2014. Physiological roles of regulated Ire1 dependent decay. *Frontiers in Genetics,* 5**,** 76-76.

COSTOYA, J. A. 2007. Functional analysis of the role of POK transcriptional repressors. *Brief Funct Genomic Proteomic,* 6**,** 8-18.

CULBRETH, M. & ASCHNER, M. 2018. GSK-3β, a double-edged sword in Nrf2 regulation: Implications for neurological dysfunction and disease. *F1000Research,* 7**,** 1043-1043.

CULLINAN, S. B. & DIEHL, J. A. 2006. Coordination of ER and oxidative stress signaling: The PERK/Nrf2 signaling pathway. *The International Journal of Biochemistry & Cell Biology,* 38**,** 317-332.

DE LA COVA, C., ABRIL, M., BELLOSTA, P., GALLANT, P. & JOHNSTON, L. A. 2004. Drosophila myc regulates organ size by inducing cell competition. *Cell,* 117**,** 107-16.

DEMAY, Y., PEROCHON, J., SZUPLEWSKI, S., MIGNOTTE, B. & GAUMER, S. 2014. The PERK pathway independently triggers apoptosis and a Rac1/Slpr/JNK/Dilp8 signaling favoring tissue homeostasis in a chronic ER stress Drosophila model. *Cell Death & Disease,* 5**,** e1452-e1452.

DÍAZ-DÍAZ, C., FERNANDEZ DE MANUEL, L., JIMENEZ-CARRETERO, D., MONTOYA, M. C., CLAVERÍA, C. & TORRES, M. 2017. Pluripotency Surveillance by Myc-Driven Competitive Elimination of Differentiating Cells. *Developmental Cell,* 42**,** 585-599.e4.

DINAN, M. 2018. Identifying a common cause of the loser cell status in Drosophila melanogaster

Thesis.

EICHENLAUB, T., COHEN, S. M. & HERRANZ, H. 2016. Cell Competition Drives the Formation of Metastatic Tumors in a Drosophila Model of Epithelial Tumor Formation. *Current Biology,* 26**,** 419-427.

FRANCIS, M. J., ROCHE, S., CHO, M. J., BEALL, E., MIN, B., PANGANIBAN, R. P. & RIO, D. C. 2016. Drosophila IRBP bZIP heterodimer binds P-element DNA and affects hybrid dysgenesis. *Proceedings of the National Academy of Sciences,* 113**,** 13003.

GREWAL, S. S., LI, L., ORIAN, A., EISENMAN, R. N. & EDGAR, B. A. 2005. Myc-dependent regulation of ribosomal RNA synthesis during Drosophila development. *Nature Cell Biology,* 7**,** 295-302.

GRONER, B. & VON MANSTEIN, V. 2017. Jak Stat signaling and cancer: Opportunities, benefits and side effects of targeted inhibition. *Mol Cell Endocrinol,* 451**,** 1-14.

HETZ, C., MARTINON, F., RODRIGUEZ, D. & GLIMCHER, L. H. 2011. The Unfolded Protein Response: Integrating Stress Signals Through the Stress Sensor IRE1α. *Physiological Reviews,* 91**,** 1219-1243.

HEYER, B. S., MACAULEY, A., BEHRENDTSEN, O. & WERB, Z. 2000. Hypersensitivity to DNA damage leads to increased apoptosis during early mouse development. *Genes & Development,* 14**,** 2072-2084.

HOLLIEN, J., LIN, J. H., LI, H., STEVENS, N., WALTER, P. & WEISSMAN, J. S. 2009. Regulated Ire1-dependent decay of messenger RNAs in mammalian cells. *Journal of Cell Biology,* 186**,** 323-331.

HUGGINS, C. J., MAYEKAR, M. K., MARTIN, N., SAYLOR, K. L., GONIT, M., JAILWALA, P., KASOJI, M., HAINES, D. C., QUIÑONES, O. A. & JOHNSON, P. F. 2015. C/EBPγ Is a Critical Regulator of Cellular Stress Response Networks through Heterodimerization with ATF4. *Mol Cell Biol,* 36**,** 693-713.

IGAKI, T., PAGLIARINI, R. A. & XU, T. 2006. Loss of Cell Polarity Drives Tumor Growth and Invasion through JNK Activation in Drosophila. *Current Biology,* 16**,** 1139-1146.

JOHNSTON, L. A., PROBER, D. A., EDGAR, B. A., EISENMAN, R. N. & GALLANT, P. 1999. Drosophila myc Regulates Cellular Growth during Development. *Cell,* 98**,** 779-790.

KALE, A., LI, W., LEE, C. H. & BAKER, N. E. 2015. Apoptotic mechanisms during competition of ribosomal protein mutant cells: roles of the initiator caspases Dronc and Dream/Strica. *Cell Death Differentiation,* 22**,** 1300-12.

KARAM, R., LOU, C.-H., KROEGER, H., HUANG, L., LIN, J. H. & WILKINSON, M. F. 2015. The unfolded protein response is shaped by the NMD pathway. *EMBO Reports,* 16**,** 599-609.

KELLY, K. F. & DANIEL, J. M. 2006. POZ for effect POZ-ZF transcription factors in cancer and development. *Trends in Cell Biology,* 16**,** 578-587.

KIM, I., XU, W. & REED, J. C. 2008. Cell death and endoplasmic reticulum stress: disease relevance and therapeutic opportunities. *Nature Reviews Drug Discovery,* 7**,** 1013-1030.

KUCINSKI, I., DINAN, M., KOLAHGAR, G. & PIDDINI, E. 2017. Chronic activation of JNK JAK/STAT and oxidative stress signalling causes the loser cell status. *Nature Communications,* 8**,** 136.

LEE, C.-H., KIPARAKI, M., BLANCO, J., FOLGADO, V., JI, Z., KUMAR, A., RIMESSO, G. & BAKER, N. E. 2018. A Regulatory Response to Ribosomal Protein Mutations Controls Translation, Growth, and Cell Competition. *Developmental Cell,* 46**,** 456-469.e4.

LEE, T. 2014. Generating mosaics for lineage analysis in flies. *Wiley Interdisciplinary Reviews. Developmental Biology,* 3**,** 69-81.

LI, W. & BAKER, N. E. 2007. Engulfment Is Required for Cell Competition. *Cell,* 129**,** 1215-1225.

MADAN, E., PELHAM, C. J., NAGANE, M., PARKER, T. M., CANAS-MARQUES, R., FAZIO, K., SHAIK, K., YUAN, Y., HENRIQUES, V., GALZERANO, A., YAMASHITA, T., PINTO, M. A. F., PALMA, A. M., CAMACHO, D., VIEIRA, A., SOLDINI, D., NAKSHATRI, H., POST, S. R., RHINER, C., YAMASHITA, H., ACCARDI, D., HANSEN, L. A., CARVALHO, C., BELTRAN, A. L., KUPPUSAMY, P., GOGNA, R. & MORENO, E. 2019. Flower isoforms promote competitive growth in cancer. *Nature,* 572**,** 260-264.

MALLIK, M., CATINOZZI, M., HUG, C. B., ZHANG, L., WAGNER, M., BUSSMANN, J., BITTERN, J., MERSMANN, S., KLÄMBT, C., DREXLER, H. C. A., HUYNEN, M. A., VAQUERIZAS, J. M. & STORKEBAUM, E. 2018. Xrp1 genetically interacts with the ALS-associated FUS orthologue caz and mediates its toxicity. *The Journal of Cell biology,* 217**,** 3947-3964.

MANOVA, K., TOMIHARA-NEWBERGER, C., WANG, S., GODELMAN, A., KALANTRY, S., WITTY-BLEASE, K., DE LEON, V., CHEN, W. S., LACY, E. & BACHVAROVA, R. F. 1998. Apoptosis in mouse embryos: elevated levels in pregastrulae and in the distal anterior region of gastrulae of normal and mutant mice. *Dev Dyn,* 213**,** 293-308.

MARUSYK, A., PORTER, C. C., ZABEREZHNYY, V. & DEGREGORI, J. 2010. Irradiation selects for p53-deficient hematopoietic progenitors. *PLoS biology,* 8**,** e1000324-e1000324.

MARYGOLD, S. J., ROOTE, J., REUTER, G., LAMBERTSSON, A., ASHBURNER, M., MILLBURN, G. H., HARRISON, P. M., YU, Z., KENMOCHI, N., KAUFMAN, T. C., LEEVERS, S. J. & COOK, K. R. 2007. The ribosomal protein genes and Minute loci of Drosophila melanogaster. *Genome biology,* 8**,** R216-R216.

MATAMORO-VIDAL, A. & LEVAYER, R. 2019. Multiple Influences of Mechanical Forces on Cell Competition. *Current Biology,* 29**,** R762-R774.

MENDELL, J. T., SHARIFI, N. A., MEYERS, J. L., MARTINEZ-MURILLO, F. & DIETZ, H. C. 2004. Nonsense surveillance regulates expression of diverse classes of mammalian transcripts and mutes genomic noise. *Nat Genet,* 36**,** 1073-8.

METZSTEIN, M. M. & KRASNOW, M. A. 2006. Functions of the nonsense-mediated mRNA decay pathway in Drosophila development. *PLoS genetics,* 2**,** e180-e180.

MORATA, G. & RIPOLL, P. 1975. Minutes: Mutants of Drosophila autonomously affecting cell division rate. *Developmental Biology,* 42**,** 211-221.

MORENO, E. & BASLER, K. 2004. dMyc Transforms Cells into Super-Competitors. *Cell,* 117**,** 117-129.

MORENO, E., BASLER, K. & MORATA, G. 2002. Cells compete for Decapentaplegic survival factor to prevent apoptosis in Drosophila wing development. *Nature,* 416**,** 755-759.

NELSON, J. O., MOORE, K. A., CHAPIN, A., HOLLIEN, J. & METZSTEIN, M. M. 2016. Degradation of Gadd45 mRNA by nonsense-mediated decay is essential for viability. *eLife,* 5**,** e12876.

NETO-SILVA, R. M., DE BECO, S. & JOHNSTON, L. A. 2010. Evidence for a growth-stabilizing regulatory feedback mechanism between Myc and Yorkie, the Drosophila homolog of Yap. *Dev Cell,* 19**,** 507-20.

NORMAN, M., WISNIEWSKA, K. A., LAWRENSON, K., GARCIA-MIRANDA, P., TADA, M., KAJITA, M., MANO, H., ISHIKAWA, S., IKEGAWA, M., SHIMADA, T. & FUJITA, Y. 2012. Loss of Scribble causes cell competition in mammalian cells. *Journal of Cell Science,* 125**,** 59-66.

OLIVER, E. R., SAUNDERS, T. L., TARLÉ, S. A. & GLASER, T. 2004. Ribosomal protein L24 defect in belly spot and tail (Bst), a mouse Minute. *Development (Cambridge, England),* 131**,** 3907-3920.

PAKOS-ZEBRUCKA, K., KORYGA, I., MNICH, K., LJUJIC, M., SAMALI, A. & GORMAN, A. M. 2016. The integrated stress response. *EMBO reports,* 17**,** 1374-1395.

PÉREZ, E., LINDBLAD, J. L. & BERGMANN, A. 2017. Tumor-promoting function of apoptotic caspases by an amplification loop involving ROS, macrophages and JNK in Drosophila. *eLife,* 6**,** e26747.

PFAFFL, M. W. 2001. A new mathematical model for relative quantification in real-time RT-PCR. *Nucleic acids research,* 29**,** e45-e45.

PINAL, N., CALLEJA, M. & MORATA, G. 2019. Pro-apoptotic and pro-proliferation functions of the JNK pathway of Drosophila: roles in cell competition, tumorigenesis and regeneration. *Open Biol,* 9**,** 180256.

REINKE, A. W., BAEK, J., ASHENBERG, O. & KEATING, A. E. 2013. Networks of bZIP Protein-Protein Interactions Diversified Over a Billion Years of Evolution. *Science,* 340**,** 730.

RODRIGUES, A. B., ZORANOVIC, T., AYALA-CAMARGO, A., GREWAL, S., REYES-ROBLES, T., KRASNY, M., WU, D. C., JOHNSTON, L. A. & BACH, E. A. 2012. Activated STAT regulates growth and induces competitive interactions independently of Myc, Yorkie, Wingless and ribosome biogenesis. *Development,* 139**,** 4051.

ROZPEDEK, W., PYTEL, D., MUCHA, B., LESZCZYNSKA, H., DIEHL, J. A. & MAJSTEREK, I. 2016. The Role of the PERK/eIF2α/ATF4/CHOP Signaling Pathway in Tumor Progression During Endoplasmic Reticulum Stress. *Current molecular medicine,* 16**,** 533-544.

SANCHO, M., DI-GREGORIO, A., GEORGE, N., POZZI, S., SÁNCHEZ, JUAN M., PERNAUTE, B. & RODRÍGUEZ, TRISTAN A. 2013. Competitive Interactions Eliminate Unfit Embryonic Stem Cells at the Onset of Differentiation. *Developmental Cell,* 26**,** 19-30.

SCHINDELIN, J., ARGANDA-CARRERAS, I., FRISE, E., KAYNIG, V., LONGAIR, M., PIETZSCH, T., PREIBISCH, S., RUEDEN, C., SAALFELD, S., SCHMID, B., TINEVEZ, J.-Y., WHITE, D. J., HARTENSTEIN, V., ELICEIRI, K., TOMANCAK, P. & CARDONA, A. 2012. Fiji: an open-source platform for biological-image analysis. *Nature Methods,* 9**,** 676-682.

SIMPSON, P. & MORATA, G. 1981. Differential mitotic rates and patterns of growth in compartments in the Drosophila wing. *Developmental Biology,* 85**,** 299-308.

SUIJKERBUIJK, S. J., KOLAHGAR, G., KUCINSKI, I. & PIDDINI, E. 2016. Cell Competition Drives the Growth of Intestinal Adenomas in Drosophila. *Curr Biol,* 26**,** 428-38.

SYKIOTIS, G. P. & BOHMANN, D. 2008. Keap1/Nrf2 signaling regulates oxidative stress tolerance and lifespan in Drosophila. *Dev Cell,* 14**,** 76-85.

TAKEUCHI, A. 2019. Investigating the molecular mechanisms of cell

competition in Drosophila Melanogaster. *Thesis*.

TURKEL, N., SAHOTA, V. K., BOLDEN, J. E., GOULDING, K. R., DOGGETT, K., WILLOUGHBY, L. F., BLANCO, E., MARTIN-BLANCO, E., COROMINAS, M., ELLUL, J., AIGAKI, T., RICHARDSON, H. E. & BRUMBY, A. M. 2013. The BTB-zinc Finger Transcription Factor Abrupt Acts as an Epithelial Oncogene in Drosophila melanogaster through Maintaining a Progenitor-like Cell State. *PLOS Genetics,* 9**,** e1003627.

URANO, F., WANG, X., BERTOLOTTI, A., ZHANG, Y., CHUNG, P., HARDING, H. P. & RON, D. 2000. Coupling of Stress in the ER to Activation of JNK Protein Kinases by Transmembrane Protein Kinase IRE1. *Science,* 287**,** 664.

USUKI, F., YAMASHITA, A. & FUJIMURA, M. 2019. Environmental stresses suppress nonsense-mediated mRNA decay (NMD) and affect cells by stabilizing NMD-targeted gene expression. *Scientific Reports,* 9**,** 1279.

VISHWAKARMA, M. & PIDDINI, E. 2020. Outcompeting cancer. *Nature Reviews Cancer,* 20**,** 187-198.

WAGSTAFF, L., GOSCHORSKA, M., KOZYRSKA, K., DUCLOS, G., KUCINSKI, I., CHESSEL, A., HAMPTON-O'NEIL, L., BRADSHAW, C. R., ALLEN, G. E., RAWLINS, E. L., SILBERZAN, P., CARAZO SALAS, R. E. & PIDDINI, E. 2016. Mechanical cell competition kills cells via induction of lethal p53 levels. *Nature Communications,* 7**,** 11373.

XU, W., BAO, P., JIANG, X., WANG, H., QIN, M., WANG, R., WANG, T., YANG, Y., LORENZINI, I., LIAO, L., SATTLER, R. & XU, J. 2019. Reactivation of nonsense-mediated mRNA decay protects against C9orf72 dipeptide-repeat neurotoxicity. *Brain,* 142**,** 1349-1364.

YE, J., KUMANOVA, M., HART, L. S., SLOANE, K., ZHANG, H., DE PANIS, D. N., BOBROVNIKOVA-MARJON, E., DIEHL, J. A., RON, D. & KOUMENIS, C. 2010. The GCN2-ATF4 pathway is critical for tumour cell survival and proliferation in response to nutrient deprivation. *Embo J,* 29**,** 2082-96.

ZHANG, G., XIE, Y., ZHOU, Y., XIANG, C., CHEN, L., ZHANG, C., HOU, X., CHEN, J., ZONG, H. & LIU, G. 2017. p53 pathway is involved in cell competition during mouse embryogenesis. *Proceedings of the National Academy of Sciences,* 114**,** 498.

ZHOU, Q., NEAL, S. J. & PIGNONI, F. 2016. Mutant analysis by rescue gene excision: New tools for mosaic studies in Drosophila. *Genesis,* 54**,** 589-592.